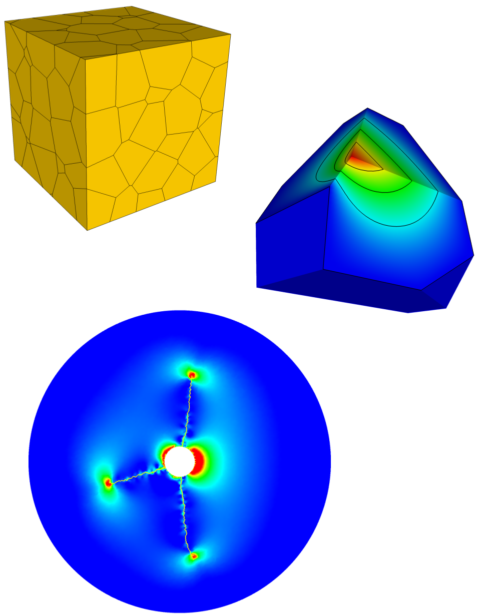

A Polyhedral Finite-Element Formulation using Harmonic Shape Functions with Applications to the Modeling of Multi-Physics Fracture Processes

Joe Bishop
Computational Structural Mechanics and Applications
Sandia National Laboratories
Albuquerque, NM

NSF Workshop on Barycentric Coordinates in Geometry Processing and Finite/Boundary Element Methods
Columbia University, New York, USA
July 25–27, 2012

This material is based upon work supported as part of the Center for Frontiers of Subsurface Energy Security, an Energy Frontier Research Center funded by the U.S. Department of Energy, Office of Science, Office of Basic Energy Sciences under Award Number DE-SC0001114.

Sandia National Laboratories

U.S. DEPARTMENT OF ENERGY

NNSA National Nuclear Security Administration

Sandia National Laboratories is a multi-program laboratory managed and operated by Sandia Corporation, a wholly owned subsidiary of Lockheed Martin Corporation, for the U.S. Department of Energy's National Nuclear Security Administration under contract DE-AC04-94AL85000.

Outline

1. Pervasive fracture and fragmentation
2. Random meshes and a polyhedral finite-element formulation
3. Assessing mesh convergence in a probabilistic sense
4. Summary

Pervasive Fracture

blast induced structural collapse

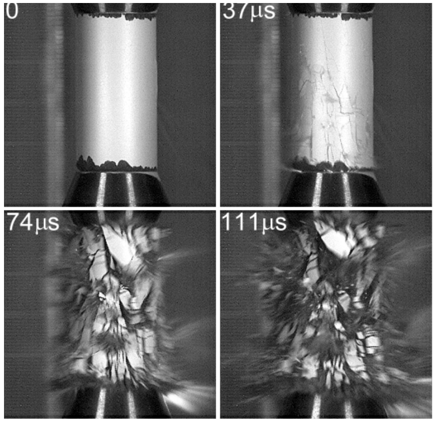

dynamic pervasive fracture

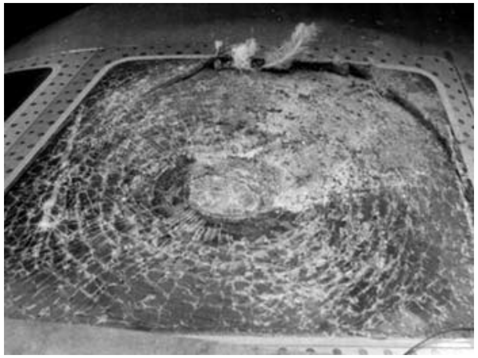

bird strike

- crack branching
- crack coalescence
- tortuous crack paths
  (sensitivity to material heterogeneity)
- stochastic behavior

Geomechanics Applications

Engineered Geothermal

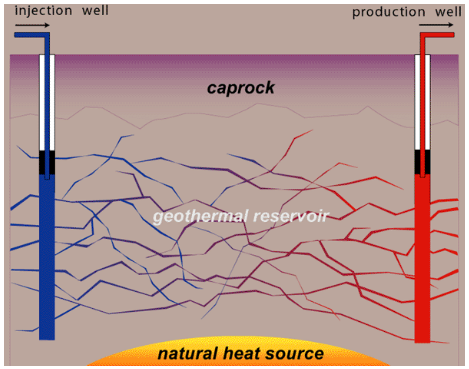

Nuclear Waste Isolation

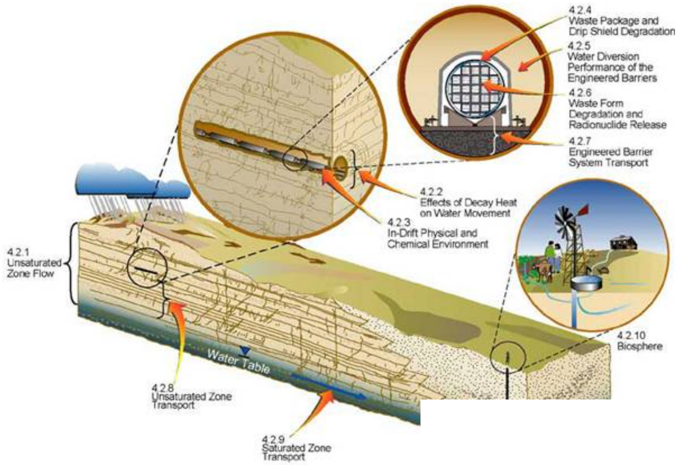

CO_2 Sequestration

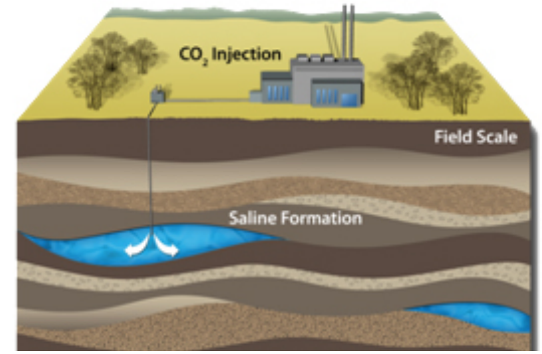

Compressed Air Energy Storage

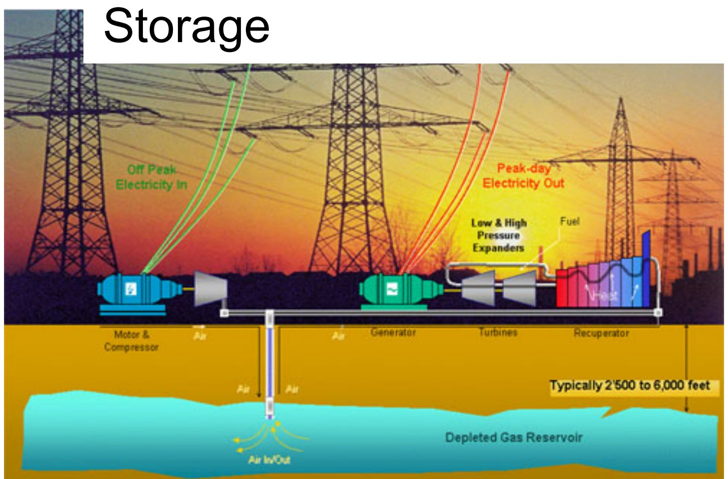

Derek Sept. 2009

Hydraulic Fracturing

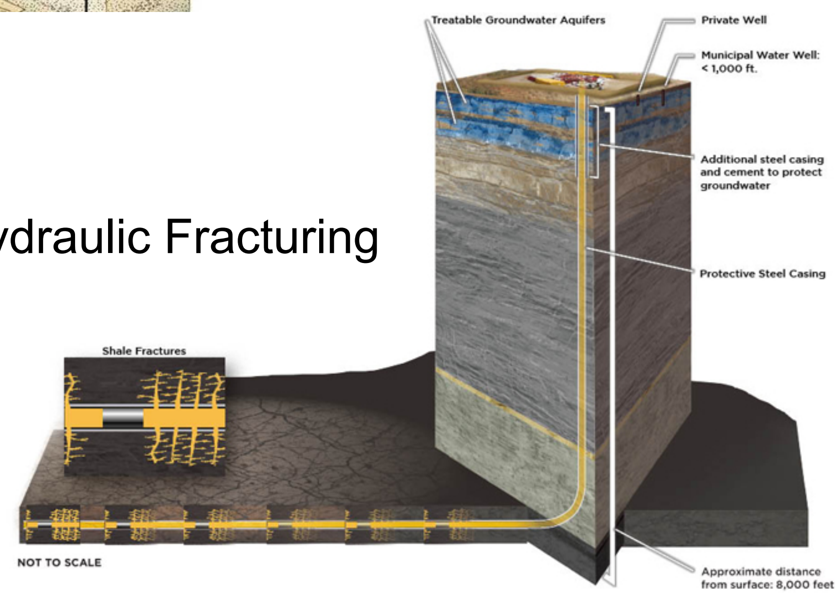

http://www.hydraulicfracturing.com

Spectrum of Fracture Problems

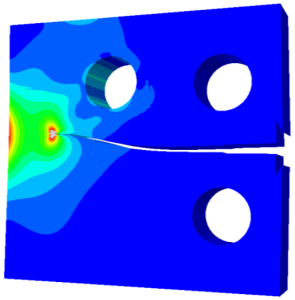

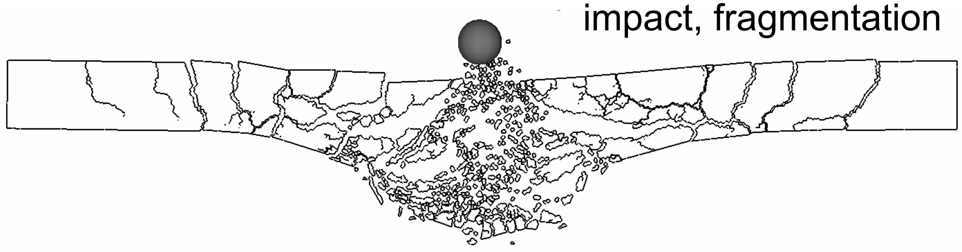

spectrum of fracture problems

single crack ⟷ pervasive fracture

- well defined deterministic propagation path
- analytical solutions
- enrichment methods (GFEM, XFEM, . . .)

- crack branching
- crack coalescence
- tortuous crack paths
  (sensitivity to material heterogeneity)
- stochastic behavior

How far can we extend the computational tools used for one end of the spectrum to the other?

Computational Challenges to Allowing Cracks to Grow Arbitrarily

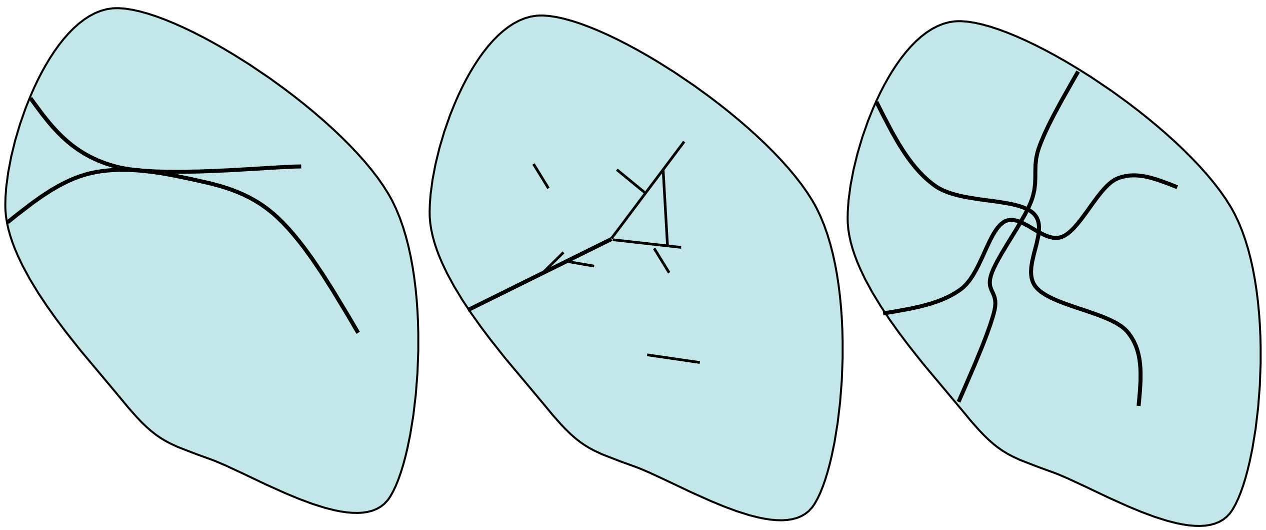

- Do we restrict branching?
- Do we restrict initiation?
  - from surface only?
  - from crack tips only?
  - from existing cracks only?
- Constraints on turning angles?
- Constraints on crossing angles?
- Constraints on minimum fragment size?

What about 3D?

Computational Approach

- Random Voronoi tessellation (mesh)
- Polyhedral finite-elements
- Fracture only allowed at element edges.
- *Dynamic* mesh connnectivity
- Insert cohesive tractions on new fracture surfaces (fracture energy).

Pandolfi, A. and M. Ortiz, 2002, *Engineering with Computers*, **18**: p. 148-159.

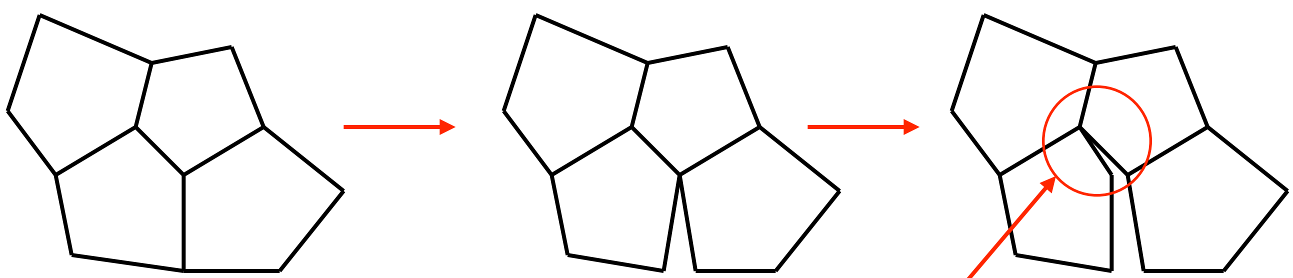

changing mesh connectivity

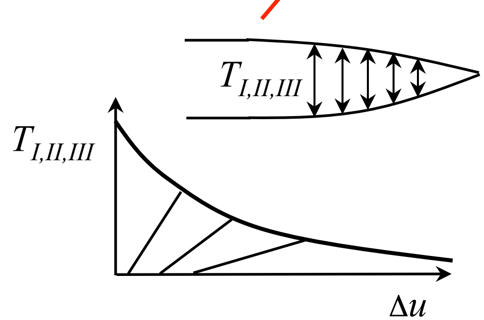

cohesive tractions at crack tip

Why a Random Voronoi Mesh?

Bolander, J.E. and S. Saito, 1998, *Fracture analyses using spring networks with random geometry.* Engineering Fracture Mechanics, **61**(5-6): p. 569-591.

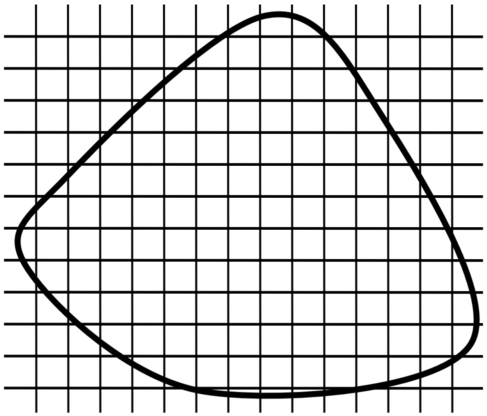

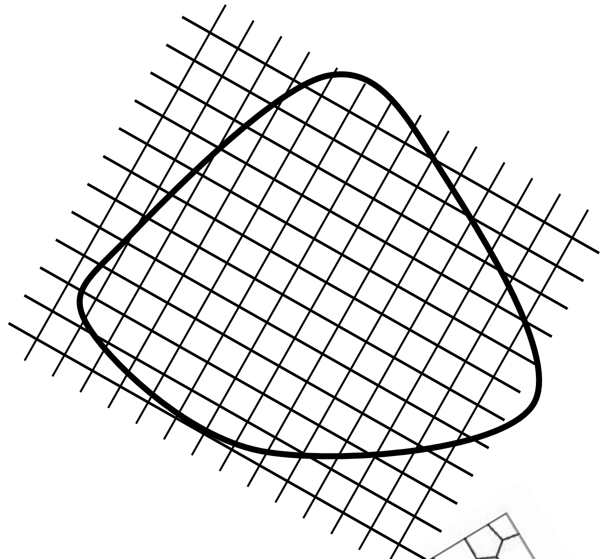

Structured grids can result in strong mesh induced bias (nonobjective).

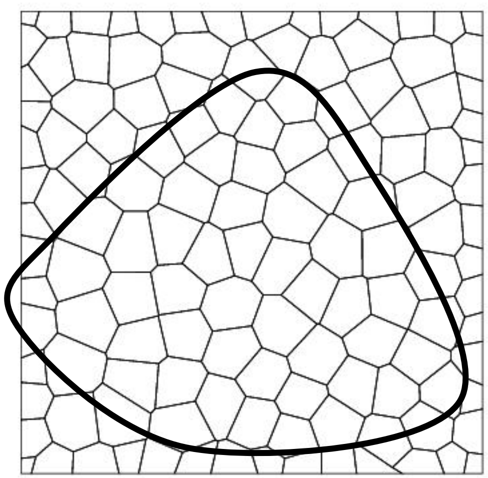

Voronoi tesselation of with random seeding

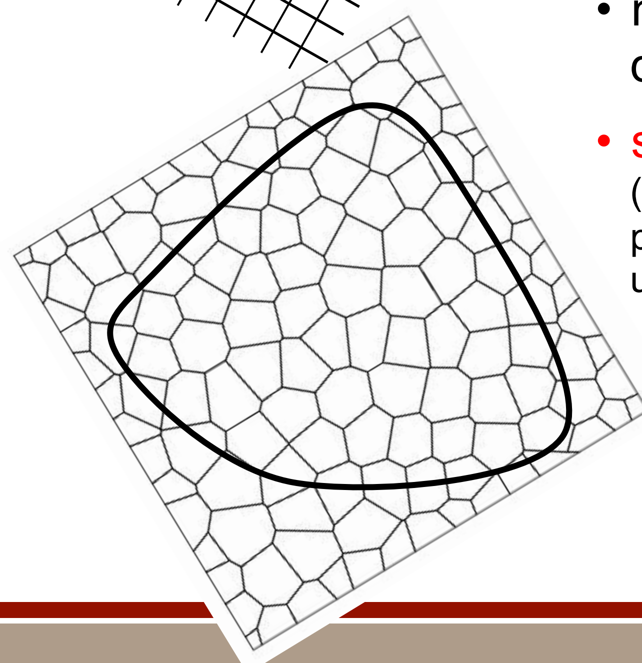

- need to use ‘random’ discretizations
- statistically isotropic
  (distribution of edge orientations passes KS test against the uniform distribution)

Voronoi Texture Augments Material Variability

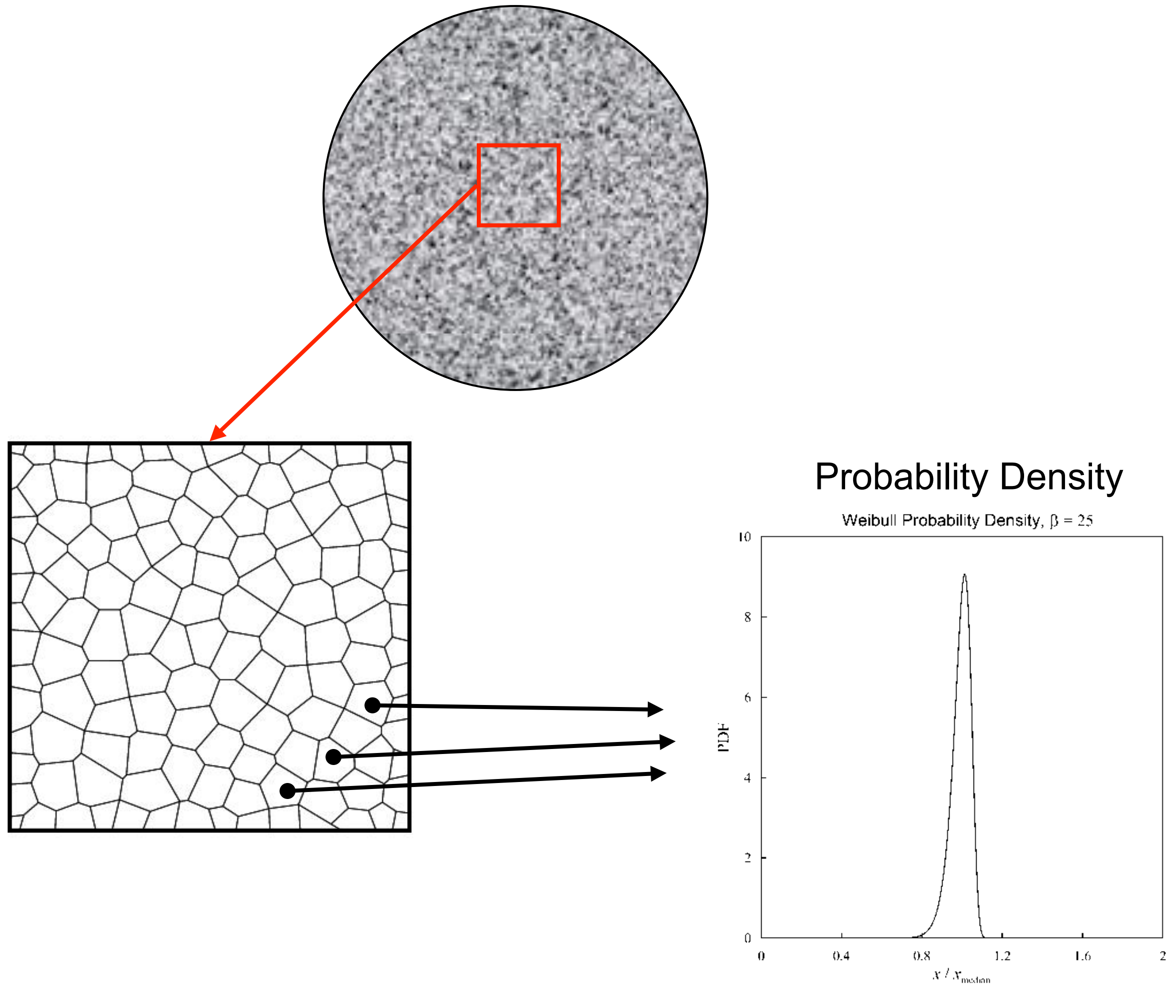

Voronoi Mesh Generation

Bolander, J., Saito, S., 1998, ‘Fracture Analyses using Spring Networks with Random Geometry,’ *Engineering Fracture Mechanics*, 61, 569-591

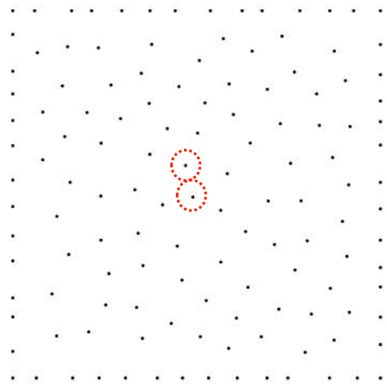

Poisson process

- constraint on min. dist.
- seed until ‘max’ packing

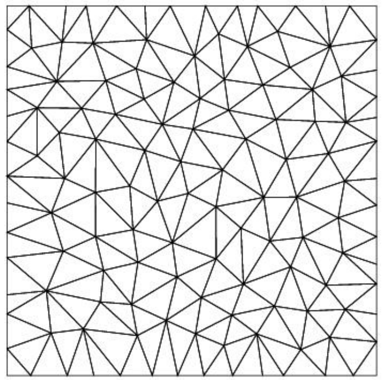

Delaunay triangulation

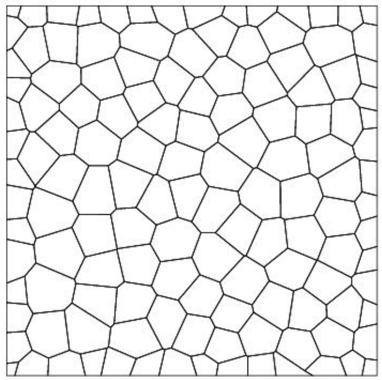

dual Voronoi

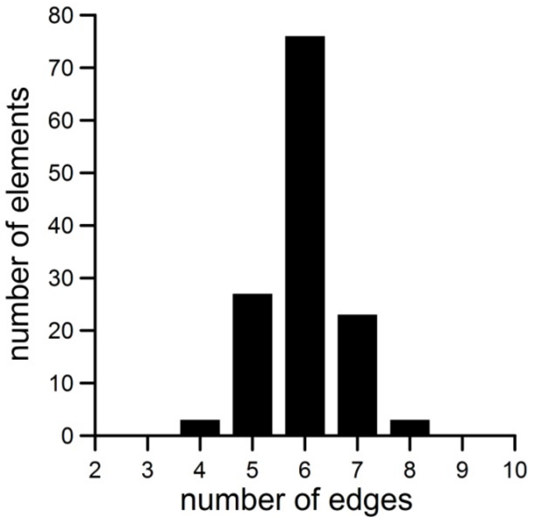

- Note that each Voronoi junction is randomly oriented.
- Most Voronoi junctions are triples.
- Average interior angles are 120°.

3D Randomly Close-Packed Voronoi

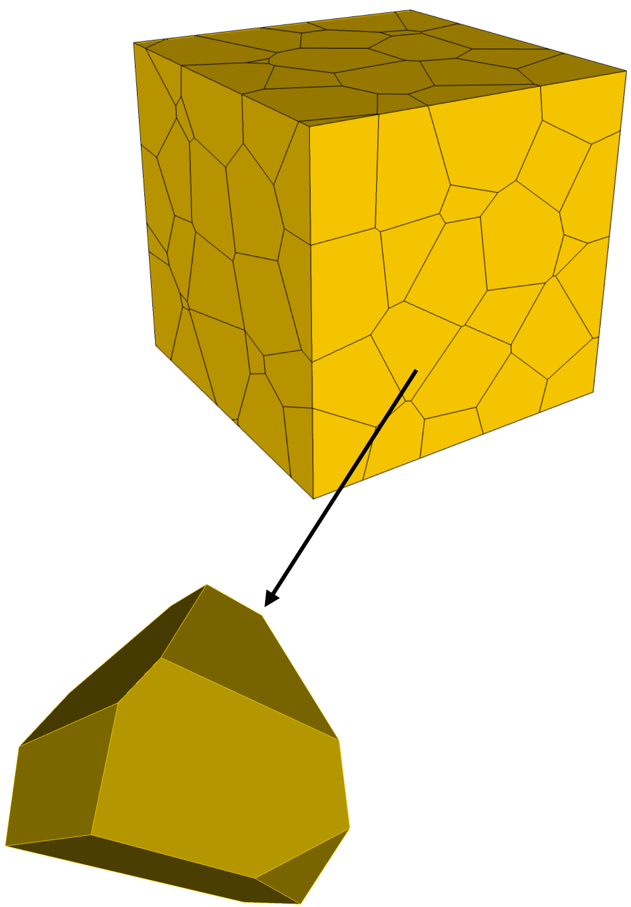

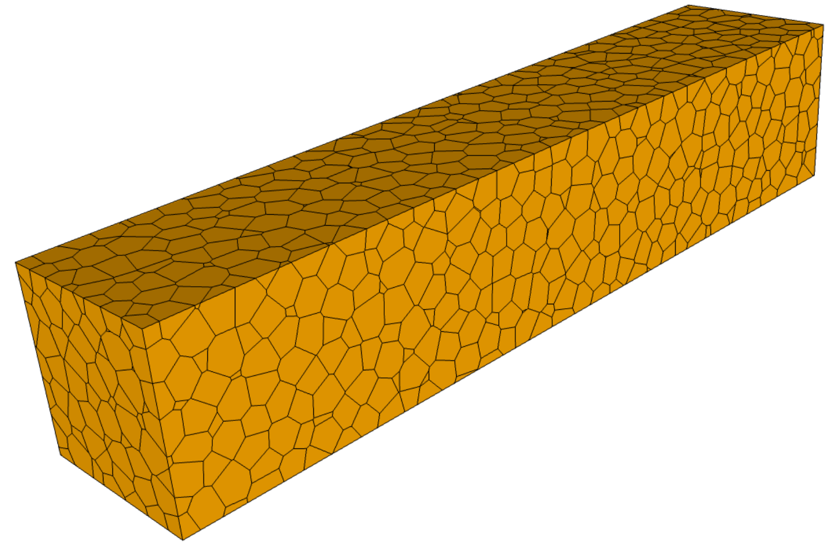

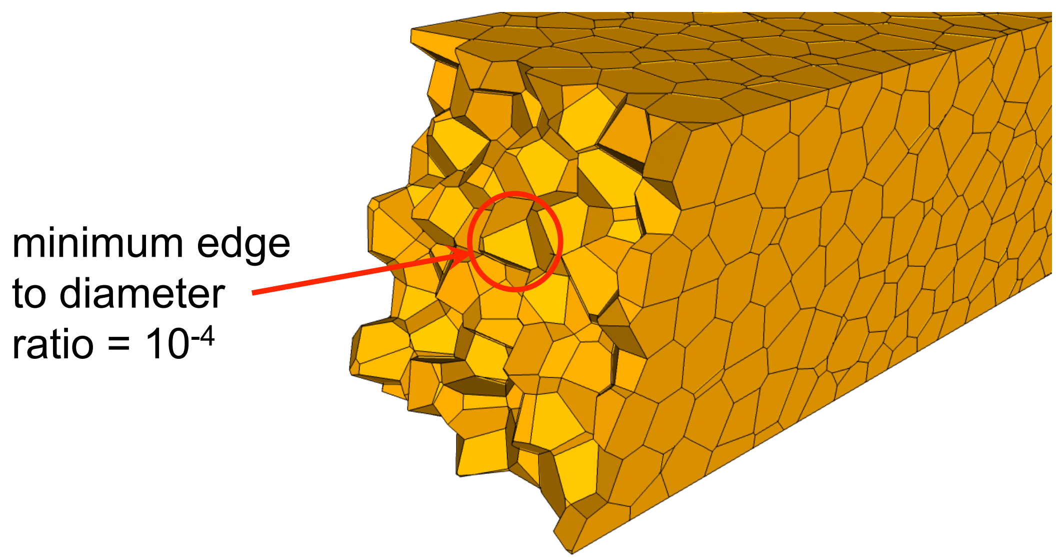

Equations of Motion

Sandia National Laboratories

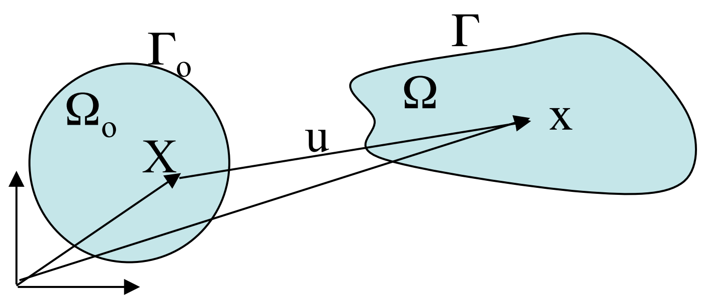

- Shape functions, their derivatives, and the integration points are defined in the initial configuration (Ω_o, Γ_o).
- All integrations of the weak form are from the original configuration (total-Lagrangian formulation).

Momentum strong form

$$\frac{\partial \mathbf{P}}{\partial \mathbf{X}} : \mathbf{I} + \rho_o \mathbf{f} = \rho_o \ddot{\mathbf{u}}$$

$\mathbf{P}$ is the first Piola-Kirchhoff stress tensor.
$\mathbf{X}$ is the position vector of a material point.
$\mathbf{x}$ is the spatial vector.
$\mathbf{u} = \mathbf{x} - \mathbf{X}$, is the displacement vector
$\mathbf{f}$ is the body force vector per unit mass.

Momentum weak form

$$\int_{\Omega_o} \rho_o \ddot{\mathbf{u}} \cdot \delta\mathbf{u}\, d\Omega_o = \int_{\Gamma_o} \mathbf{t}_o \cdot \delta\mathbf{u}\, d\Gamma_o + \int_{\Omega_o} \rho_o \mathbf{f} \cdot \delta\mathbf{u}\, d\Omega_o - \int_{\Omega_o} \rho_o \mathbf{P} : (\partial(\delta\mathbf{u})/\partial\mathbf{X})\ d\Omega_o$$

However, most material models are hypoelastic.

deformation gradient

$$F = \frac{\partial \mathbf{x}}{\partial \mathbf{X}} \quad (3\times 3)$$

rate of deformation

$$\frac{\partial \mathbf{v}}{\partial \mathbf{x}} = \frac{\partial \mathbf{v}}{\partial \mathbf{X}} F^{-1}$$

PK1 stress

$$P = J\,\sigma F^{-T}$$
$$J = \det(F)$$

Cauchy stress

$$\sigma = J^{-1} P F^{T}$$

Lots of multiplications by F and F^{-1}

Harmonic Functions

A harmonic function is a solution of Laplace's equation.

$$\nabla^2 \varphi = 0 \quad \text{or} \quad \frac{\partial^2 \varphi}{\partial x^2} + \frac{\partial^2 \varphi}{\partial y^2} + \frac{\partial^2 \varphi}{\partial z^2} = 0$$

Can solve efficiently using BEM, or can just use FEM.

example in 2D

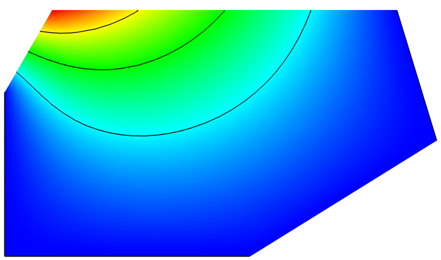

example in 3D

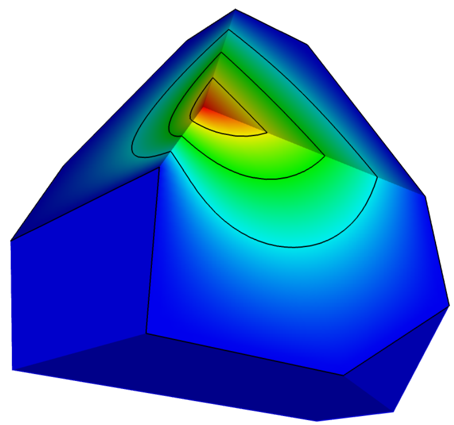

Construction of Harmonic Shape Functions in 3D

(Joshi, 2007)

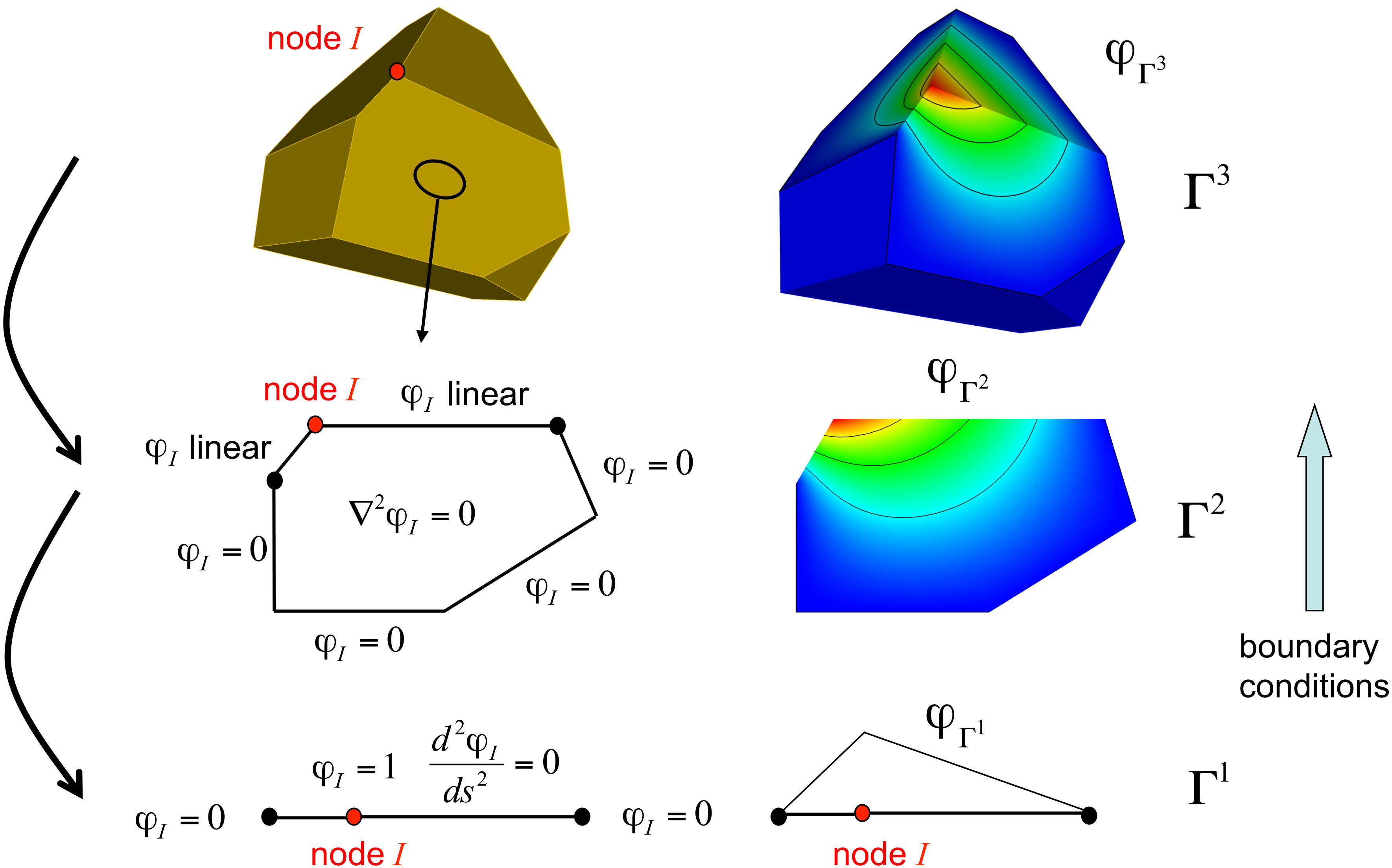

Harmonic Shape Function Properties

- partition of unity and reproduce space $\sum_I \psi_I(\mathbf{x}) = 1, \quad \sum_I \psi_I(\mathbf{x})\ \mathbf{x}_I = \mathbf{x}$

  even for the discrete harmonic solution $\sum_I \psi_I^h(\mathbf{x}) = 1, \quad \sum_I \psi_I^h(\mathbf{x})\ \mathbf{x}_I = \mathbf{x}$

- Kronecker delta property at nodes $\psi_I(\mathbf{x}_J) = \delta_{IJ}$
- shape functions defined on original configuration (no mapping to 'parent' shape)

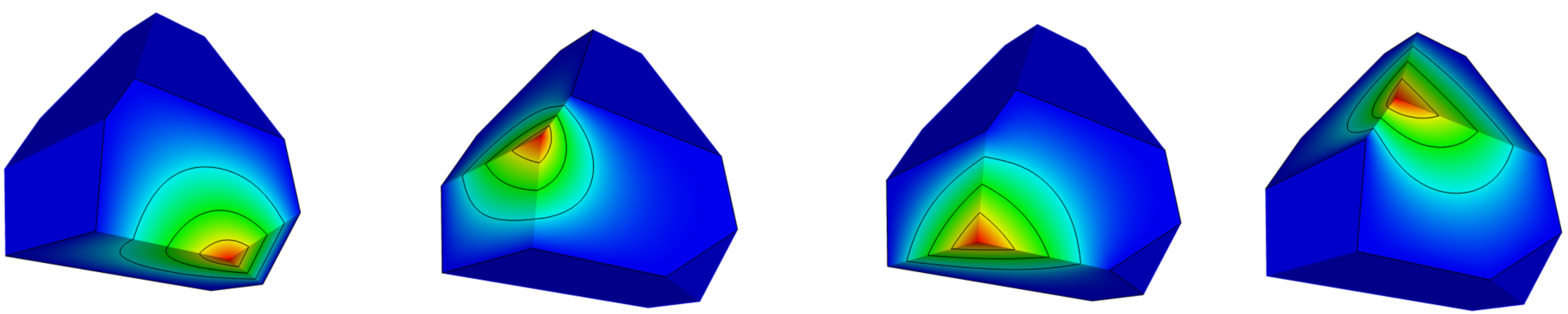

shape functions

Harmonic Shape Function Examples

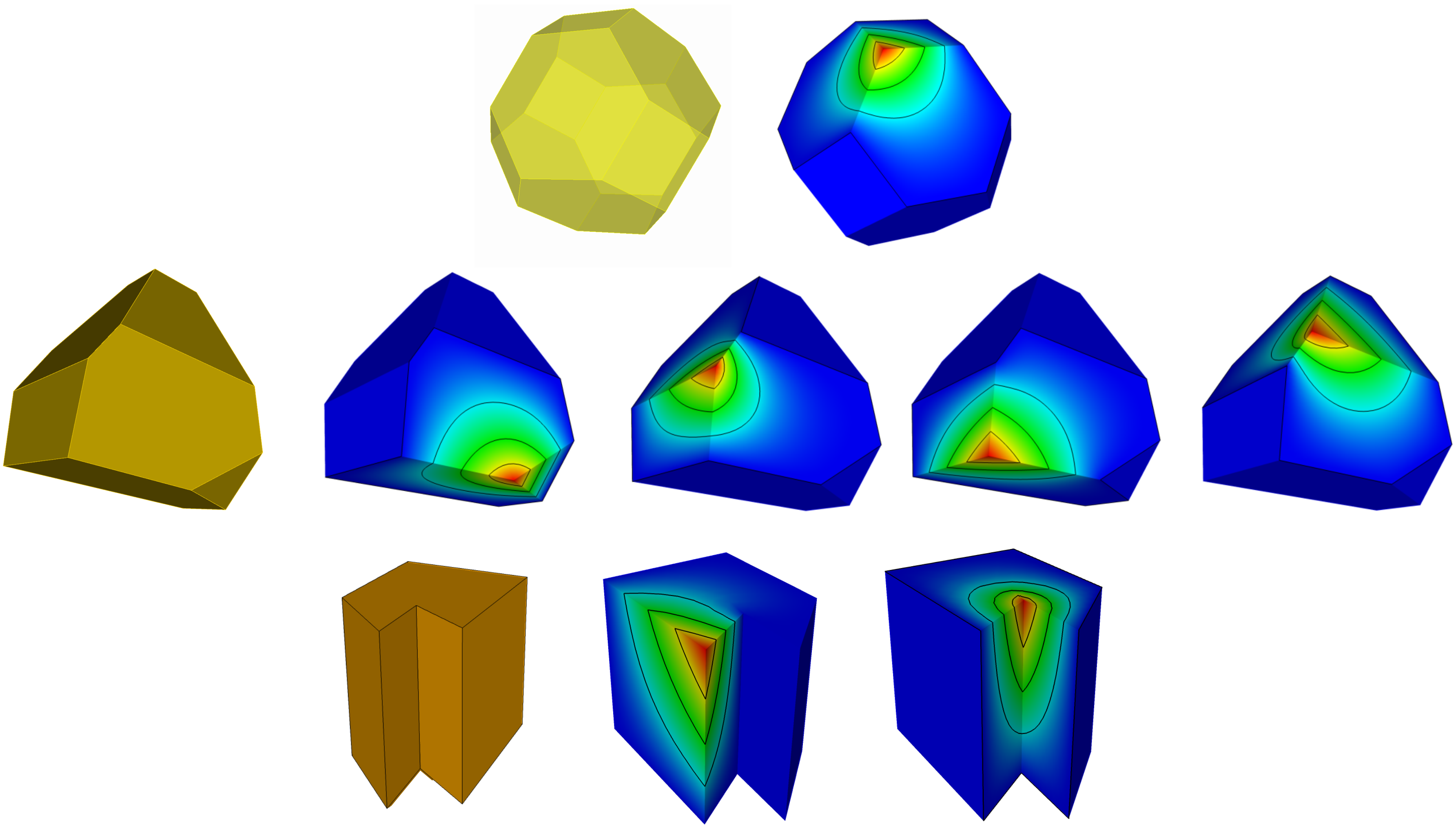

Only need to store shape functions and derivatives at integration points.
Discard everything else.

Accuracy of Harmonic Shape Functions?

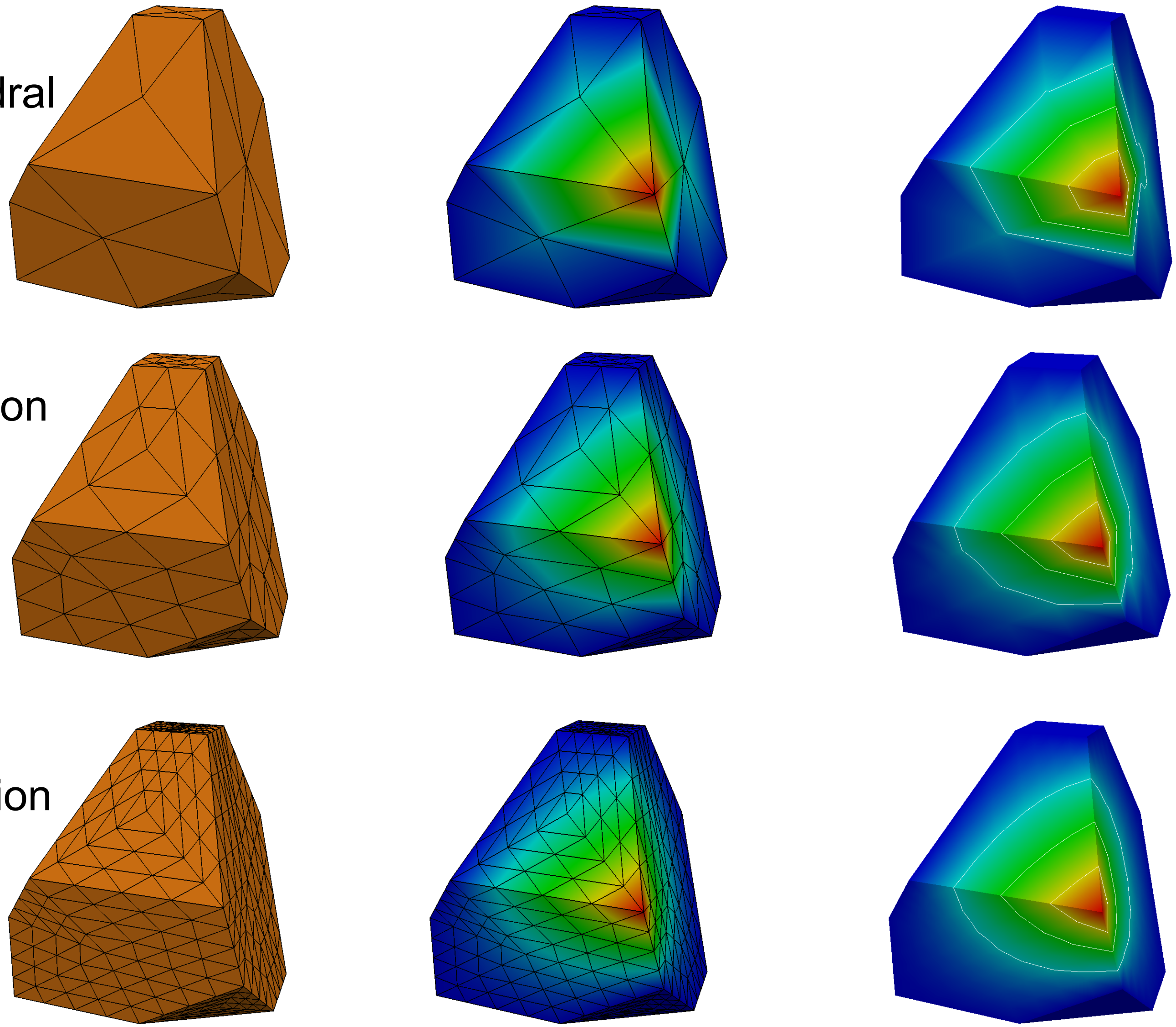

Base tetrahedral subdivision

R0

1 : 8 subdivision

R1

1 : 8 subdivision

R2

Comments and Questions

1. What accuracy is needed in the solution of the harmonic shape functions and their derivatives?
2. How to integrate the weak form?

These questions are intimately related!

Element Integration

- Due to computational expense of plasticity models, want to minimize the number of integration points.
- Follow approach of Rashid and Selimotec, 2006.
- Each node is associated with a “tributary” volume, connected to the centroid.
- Number of integration points is equal to the number of vertices.

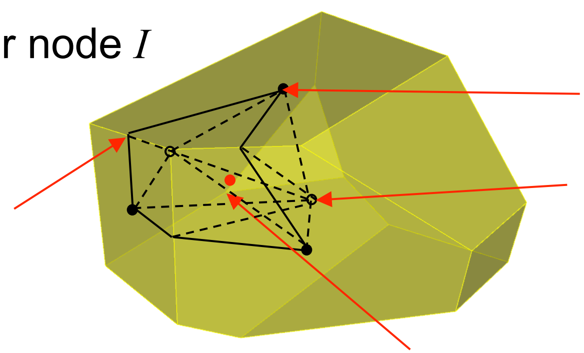

$$\int_{\Omega^e} f \, d\Omega^e \approx \sum_{k=1}^{M} w_k \, f(\mathbf{x}_k)$$

Sufficient to eliminate any zero energy modes.

“Engineering” Patch Test

The patch test verifies “completeness”, a necessary condition for convergence.

(Displacement field can represent rigid body motions and a constant strain state.)

Conversely, a constant stress field should be produced within each element when such a field is prescribed on the boundary surface.

and, strain field should be constant.

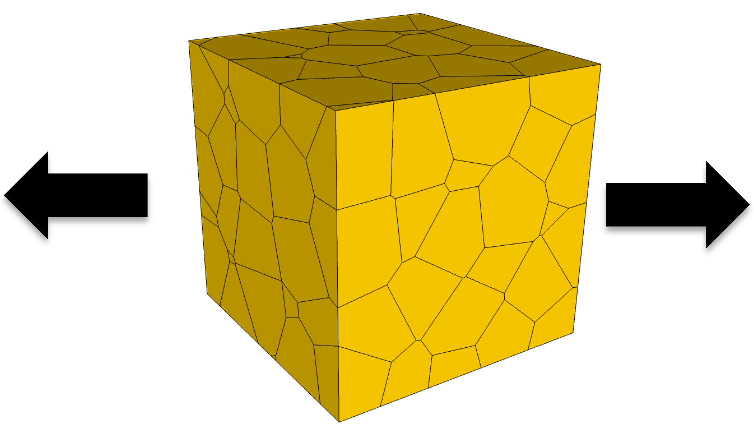

patch of elements

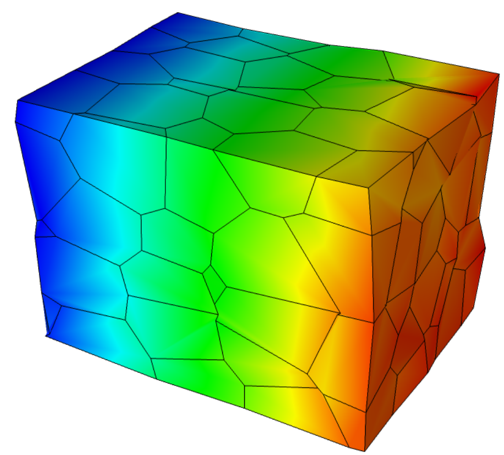

Failed patch test!

strain error ~ 20%

Element Stiffness Matrix (Linear Example)

From the weak form we get the element stiffness matrix

$$\mathbf{k}^e = \int_{\Omega^e} \mathbf{B}^T \mathbf{D} \mathbf{B} \, d\Omega$$

D contains elastic material constants.

$$\mathbf{B}_I = \begin{bmatrix} \varphi_{I,x} & 0 & 0 \\ 0 & \varphi_{I,y} & 0 \\ 0 & 0 & \varphi_{I,z} \\ 0 & \varphi_{I,z} & \varphi_{I,y} \\ \varphi_{I,z} & 0 & \varphi_{I,x} \\ \varphi_{I,y} & \varphi_{I,x} & 0 \end{bmatrix}$$

$$\mathbf{B} = \begin{bmatrix} \mathbf{B}_1 & \mathbf{B}_2 & \cdots & \mathbf{B}_I & \cdots & \mathbf{B}_{N_{en}} \end{bmatrix}$$

N_{en} = number of element nodes

$$\underbrace{\mathbf{k}^e}_{3N_{en} \times 3N_{en}} = \begin{bmatrix} \mathbf{k}^e_{11} & \mathbf{k}^e_{12} & \cdots \\ \mathbf{k}^e_{21} & \mathbf{k}^e_{22} & \cdots \\ \vdots & \vdots & \ddots \end{bmatrix}$$

nodal submatrix

$$\underbrace{\mathbf{k}^e_{IJ}}_{3\times 3} = \int_{\Omega^e} \mathbf{B}_I^T \mathbf{D} \mathbf{B}_J \, d\Omega$$

Contains terms like: $\int_{\Omega^e} \varphi_{I,x}\varphi_{J,x}\, d\Omega, \quad \int_{\Omega^e} \varphi_{I,x}\varphi_{J,y}\, d\Omega, \quad \int_{\Omega^e} \varphi_{I,x}\varphi_{J,z}\, d\Omega, \quad \cdots$

But $\int_{\Omega^e} f \, d\Omega^e \approx \sum_{k=1}^{M} w_k \, f(\mathbf{x}_k)$ What's the effect of this approx.?

Requirements to Pass the Patch Test

(Krongauz and Belytschko, 1997)

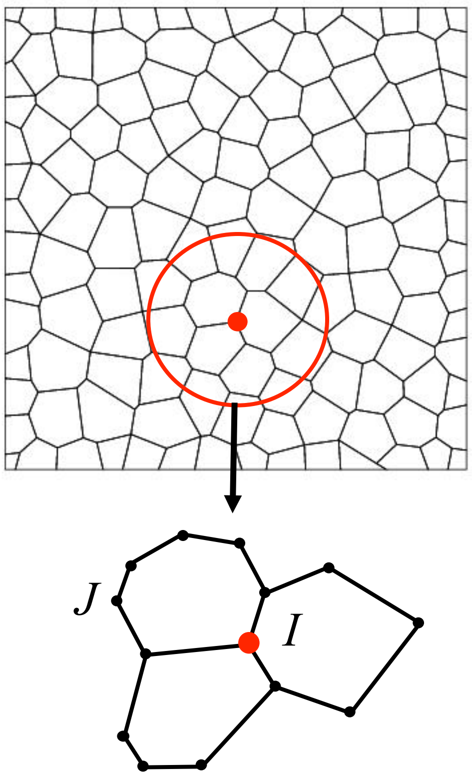

Ω_I = support of node I

global equilibrium equations: $\sum_J \mathbf{K}_{IJ}\mathbf{u}_J = \mathbf{F}_I$

K_{IJ} = global stiffness matrix

For patch test, need

$$\boxed{u_x(x,y,z) = a_1\,x + a_2\,y + a_3\,z + a_4}$$
$$u_y(x,y,z) = b_1\,x + b_2\,y + b_3\,z + b_4$$
$$u_z(x,y,z) = c_1\,x + c_2\,y + c_3\,z + c_4$$

to be a solution of $\mathrm{Ku} = \mathrm{F}$ when applied as boundary conditions.

For interior nodes I need $\sum_J \mathbf{K}_{IJ}\mathbf{u}_J^{\text{linear}} = \mathbf{0}$ $\quad (\mathbf{F}_I = 0)$

Row I column J of K_{IJ} contains terms like:

$$\int_{\Omega_I} \varphi_{I,x}\varphi_{J,x}\,d\Omega, \quad \int_{\Omega_I} \varphi_{I,x}\varphi_{J,y}\,d\Omega, \quad \int_{\Omega_I} \varphi_{I,x}\varphi_{J,z}\,d\Omega, \quad \cdots$$

For example, need $\sum_J \int_{\Omega_I} \varphi_{I,x}\varphi_{J,z}\overbrace{\left(a_1 x_J + a_2 y_J + a_3 z_J + a_4\right)}\,d\Omega = 0$

Requirements to Pass the Patch Test

(Krongauz and Belytschko, 1997)

$$\sum_J \int_{\Omega_I} \varphi_{I,x}\varphi_{J,z}\left(a_1 x_J + a_2 y_J + a_3 z_J + a_4\right) d\Omega = 0$$

$$\int_{\Omega_I} \varphi_{I,x} \sum_J \varphi_{J,z}\left(a_1 x_J + a_2 y_J + a_3 z_J + a_4\right) d\Omega = 0$$

recall $\sum_{J=1}^{N} x_J \varphi_{J,z} = 0$ $\sum_{J=1}^{N} y_J \varphi_{J,z} = 0$ $\sum_{J=1}^{N} z_J \varphi_{J,z} = 1$ and $\sum_{J=1}^{N} \varphi_{J,z} = 0$

$$\boxed{\int_{\Omega_I} \varphi_{I,x}\, d\Omega = 0}$$

similarly $\boxed{\int_{\Omega_I} \varphi_{I,y}\, d\Omega = 0}$ $\boxed{\int_{\Omega_I} \varphi_{I,z}\, d\Omega = 0}$

These integration properties of the shape function derivatives must hold in order to pass the patch test.

But what about numerical integration? $\int_{\Omega_I} \varphi_{I,x}\, d\Omega \approx \sum_{k=1}^{N_{ip}} w_k\, \varphi_{I,x}(\mathbf{x}_k)$

w_k = integration weight

x_k = integration point

Integration Consistency

Sandia National Laboratories

$\varphi_I = 0$ on Γ^I

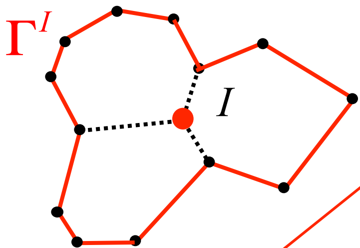

$$\int_{\Omega_I} \varphi_{I,x} \, d\Omega = 0$$

Ω_I = support of node I

is equivalent to

Divergence Theorem

$$\int_{\Omega^e} \varphi_{I,x} \, d\Omega = \int_{\Gamma^e} \varphi_I \, n_x \, d\Gamma$$

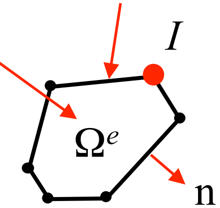

$$\int_{\Omega^e} \varphi_{I,x} \, d\Omega = \int_{\Gamma^e} \varphi_I \, n_x \, d\Gamma$$

$$\sum_{k=1}^{M} w_k \, \varphi_{I,x}(\mathbf{x}_k) \cong \sum_{j=1}^{M_\Gamma} w_j^\Gamma \, \varphi_I(\mathbf{x}_j) \, n_x(\mathbf{x}_j)$$

Satisfaction of discrete form of Divergence Theorem requires "="

Approximate integration will cause failure of patch test for first-order integration.

Would need a large number of integration points and accurate shape function derivatives to satisfy patch test.

. . . too expensive!

volume integration point at x_k with weight w_k

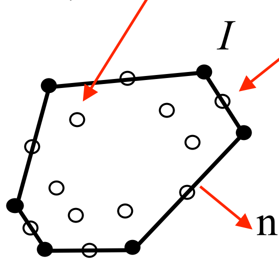

surface integration point at x_j with weight $w^\Gamma{}_j$

Instead, let's "tweak" the shape function derivatives to satisfy the patch test.

Let's "tweak" the Shape Function Derivatives

(pseudo-derivatives)

Let $a_x^{I,k}, a_y^{I,k}, a_z^{I,k}$ be the new shape function derivatives for the I-th shape function at integration point k.

How to calculate $a_x^{I,k}, a_y^{I,k}, a_z^{I,k}$?

Minimize the sum of the squares of the difference w.r.t to the original derivatives.

$$L = \sum_{I=1}^{N_{en}} \sum_{k=1}^{M} \left(\varphi_{I,x}(\mathbf{x}_k) - a_x^{I,k} \right)^2$$

with "integration constraints"

$$\sum_{k=1}^{M} w_k\, a_x^{I,k} - \sum_{j=1}^{M_\Gamma} w_j^\Gamma\, \varphi_I(\mathbf{x}_j)\, n_x(\mathbf{x}_j) = 0 \qquad I = 1, \ldots, N_{en}$$

solve use Lagrange multipliers

Modified Shape Function Derivatives

Introduce Lagrange multipliers λ_I , $I = 1, \ldots,$
N_{en} and form the augmented Lagrangian L_A

$$L_A = \sum_{I=1}^{N_{en}} \sum_{k=1}^{M} \left(\varphi_{I,x}(\mathbf{x}_k) - a_x^{I,k} \right)^2 + \sum_{i=1}^{N_{en}} \lambda_I \left[\sum_{k=1}^{M} w_k \, a_x^{I,k} - \sum_{j=1}^{M_\Gamma} w_j^\Gamma \, \varphi_I(\mathbf{x}_j) n_x(\mathbf{x}_j) \right]$$

necessary condition for local minimum

$$\frac{\partial L_A}{\partial a_x^{I,k}} = 0 \, , \quad I = 1, \cdots, N_{en} \, , \quad k = 1, \cdots, M$$

$$\frac{\partial L_A}{\partial \lambda_I} = 0 \, , \quad I = 1, \cdots, N_{en}$$

$$\underbrace{\begin{bmatrix} \mathbf{A} & \mathbf{L}^T \\ \mathbf{L} & 0 \end{bmatrix}}_{} \begin{bmatrix} \boldsymbol{a}_x \\ \boldsymbol{\lambda} \end{bmatrix} = \begin{bmatrix} \mathbf{b}_x \\ \mathbf{c}_x \end{bmatrix}$$

same for $(\ )_y$ and $(\ )_z$, only need to factor once for each element

3D Verification: Engineering Patch Test

random patch

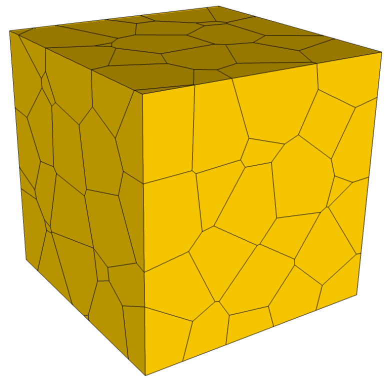

without derivative correction

with derivative correction

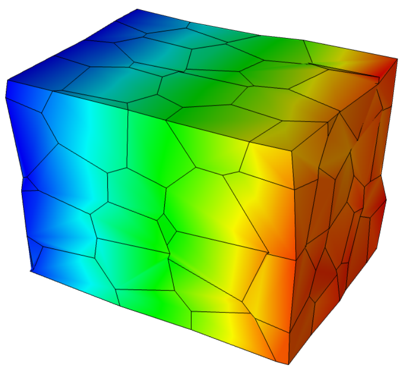

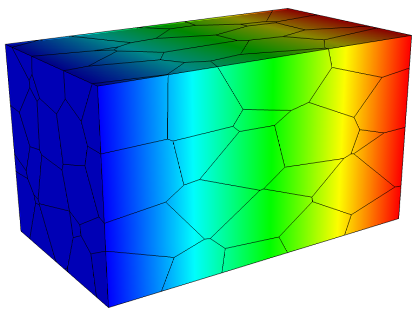

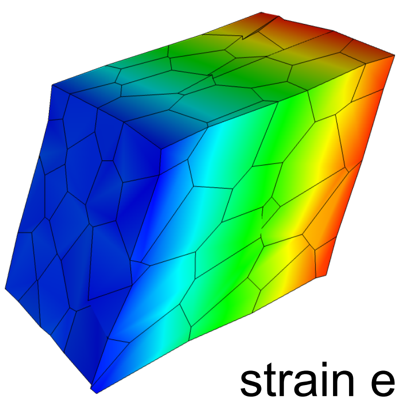

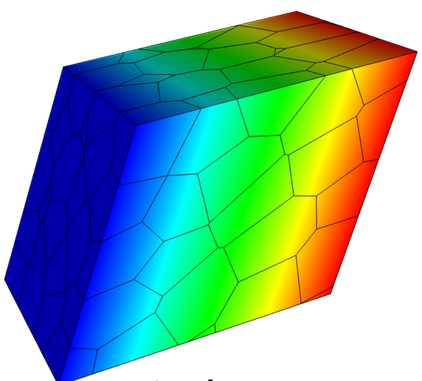

strain error = $O(10^{-1})$

strain error = $O(10^{-8})$

Patch Test with Nonconvex Elements

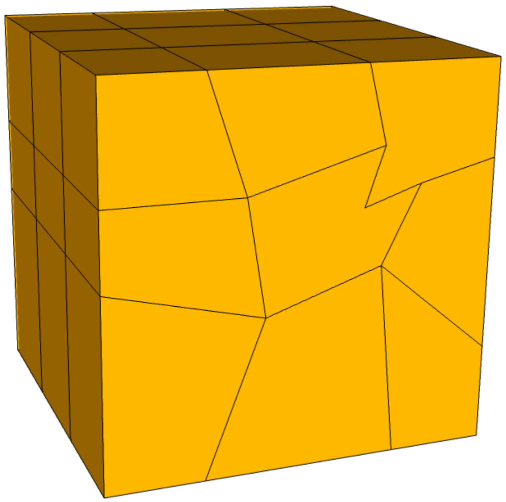

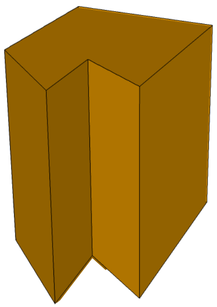

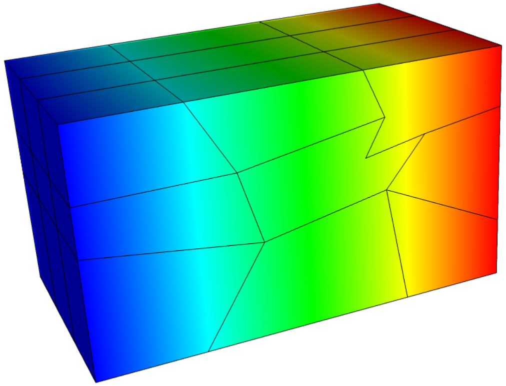

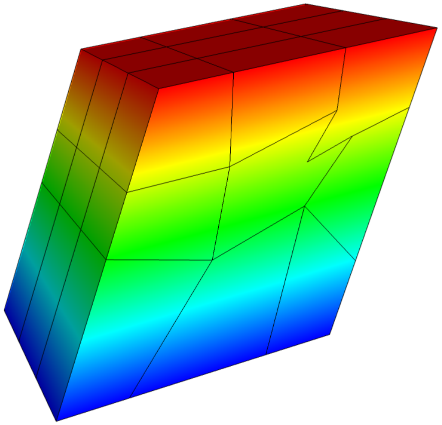

Verification Test: Beam with a Transverse End-Load

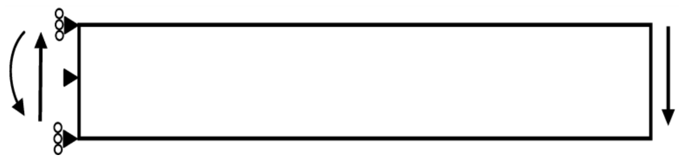

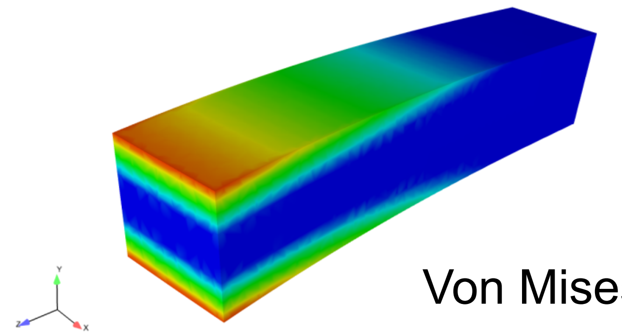

Von Mises stress field

3D exact linear elasticity solution, (Barber, 2010)

$$
\begin{aligned}
\sigma_{xx} &= \sigma_{yy} = \sigma_{xy} = 0 \\
\sigma_{zz} &= \frac{F_y}{I_x} yz \\
\sigma_{xz} &= \frac{2F_y a^2}{\pi^2 I_x} \frac{\nu}{1+\nu} \sum_{n=1}^{\infty} \frac{(-1)^n}{n^2} \sin\left(\frac{n\pi x}{a}\right) \frac{\sinh\left(\frac{n\pi y}{a}\right)}{\cosh\left(\frac{n\pi b}{a}\right)} \\
\sigma_{yz} &= \frac{F_y}{I_x} \left\{ \frac{1}{2}(b^2 - y^2) + \frac{1}{6}(3x^2 - a^2)\frac{\nu}{1+\nu} - \frac{2a^2}{\pi^2}\frac{\nu}{1+\nu} \sum_{n=1}^{\infty} \frac{(-1)^n}{n^2} \sin\left(\frac{n\pi x}{a}\right) \frac{\sinh\left(\frac{n\pi y}{a}\right)}{\cosh\left(\frac{n\pi b}{a}\right)} \right\}
\end{aligned}
$$

From this stress field → strain field → integrate to get displacement field using compatibility equations.

Randomly Close-Packed Voronoi Meshes

beam dimension = $1 \times 1 \times 5$

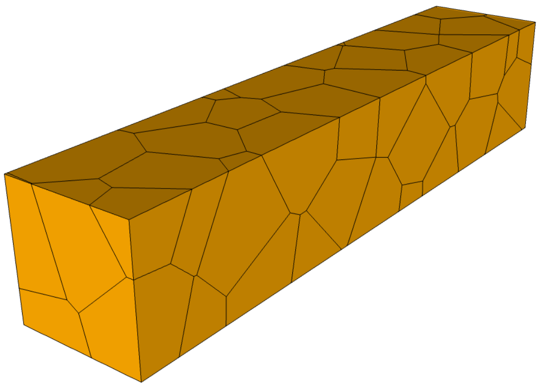

point spacing = 0.5

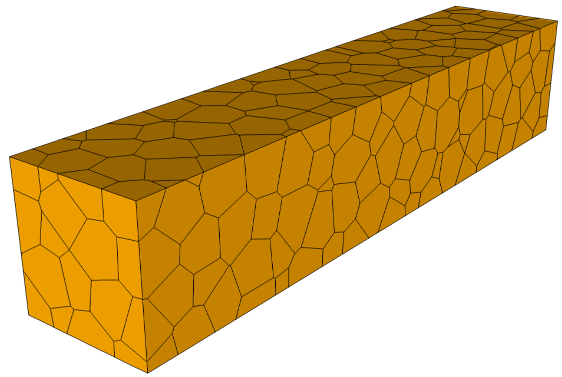

point spacing = 0.25

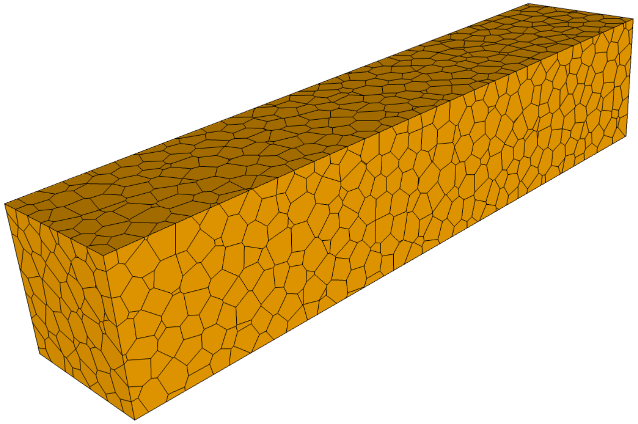

point spacing = 0.125

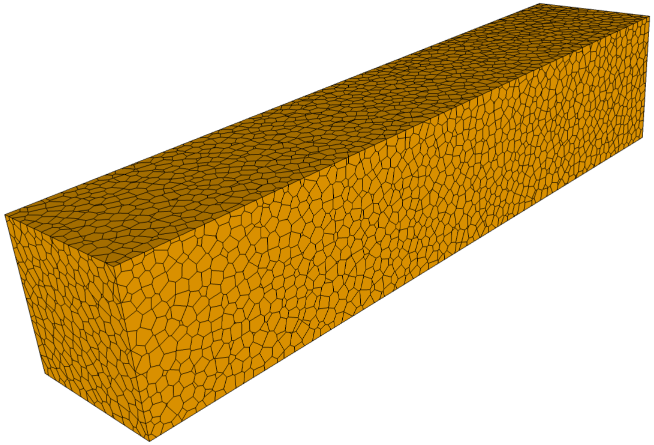

point spacing = 0.0625

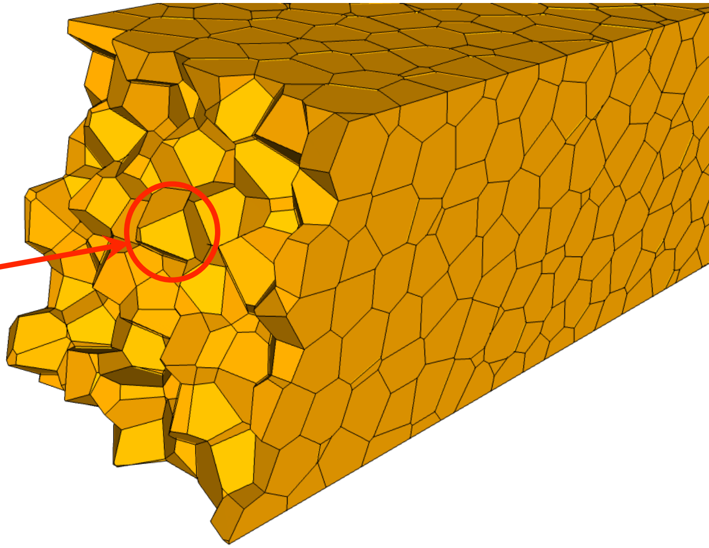

minimum edge to diameter ratio = 10^{-4}

Randomly Close-Packed Voronoi Meshes

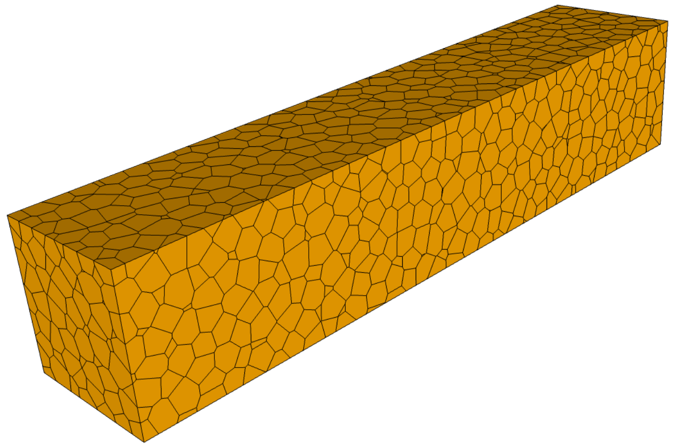

mesh statistics

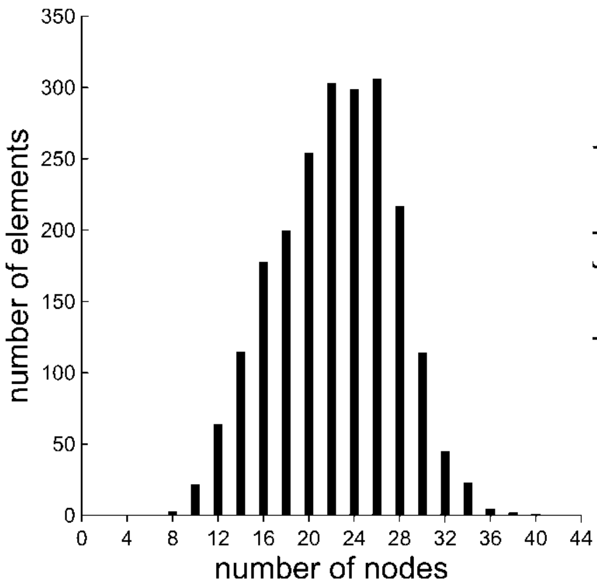

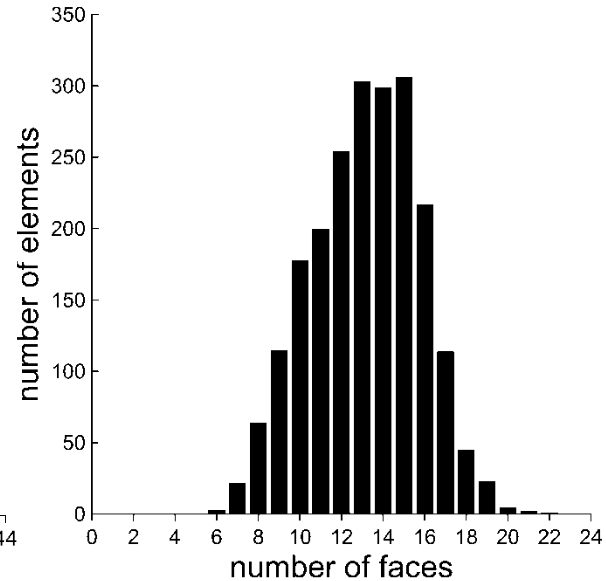

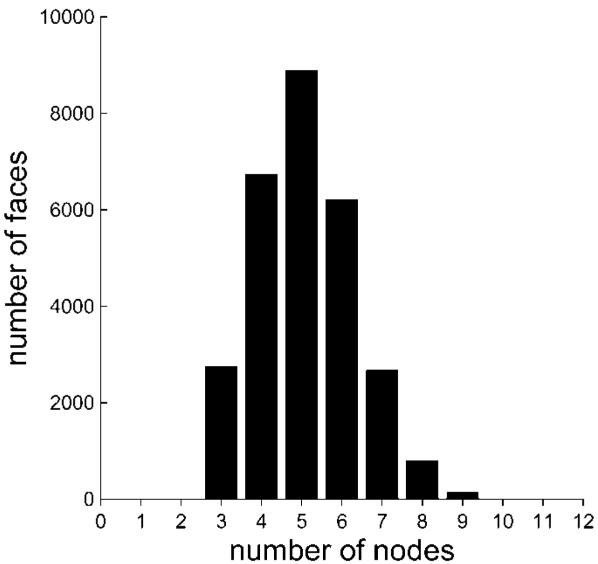

median 24 nodes per element median 14 faces per element median 5 nodes per face

Typical FEM Solution

deformed shape, Von Mises stress

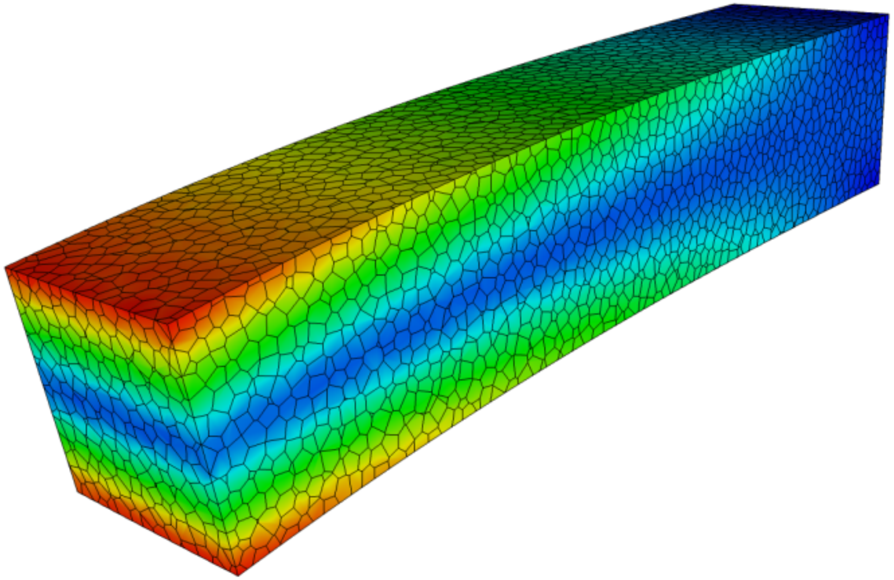

Verification Test: Beam with a Transverse End-Load

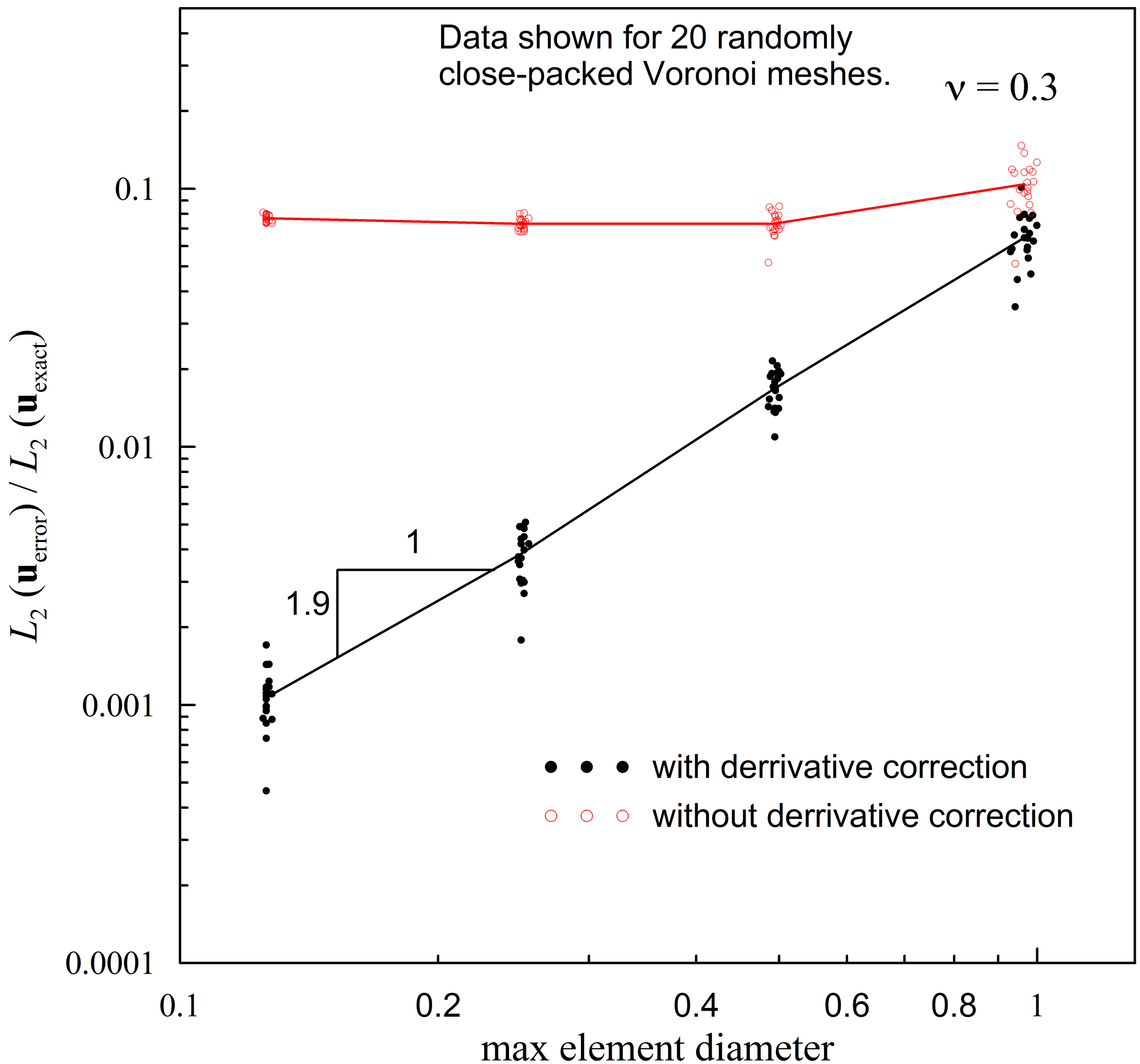

Verification Test: Beam with a Transverse End-Load

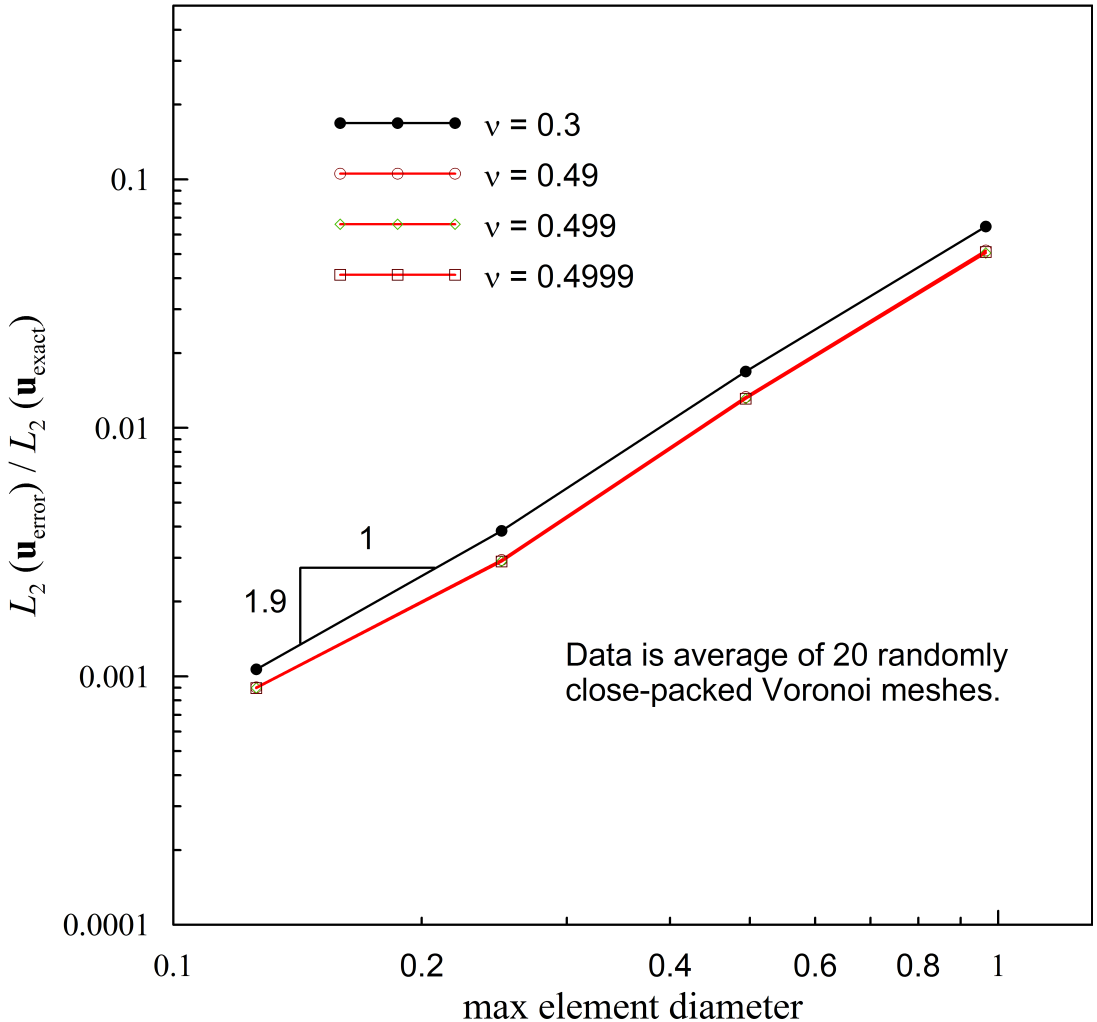

Standard mean-dilation formulation for nearly incompressible behavior (Nagtegaal, 1974)

No reduction in convergence rate as $\nu \rightarrow 1/2$.

Effect of Shape Function Accuracy

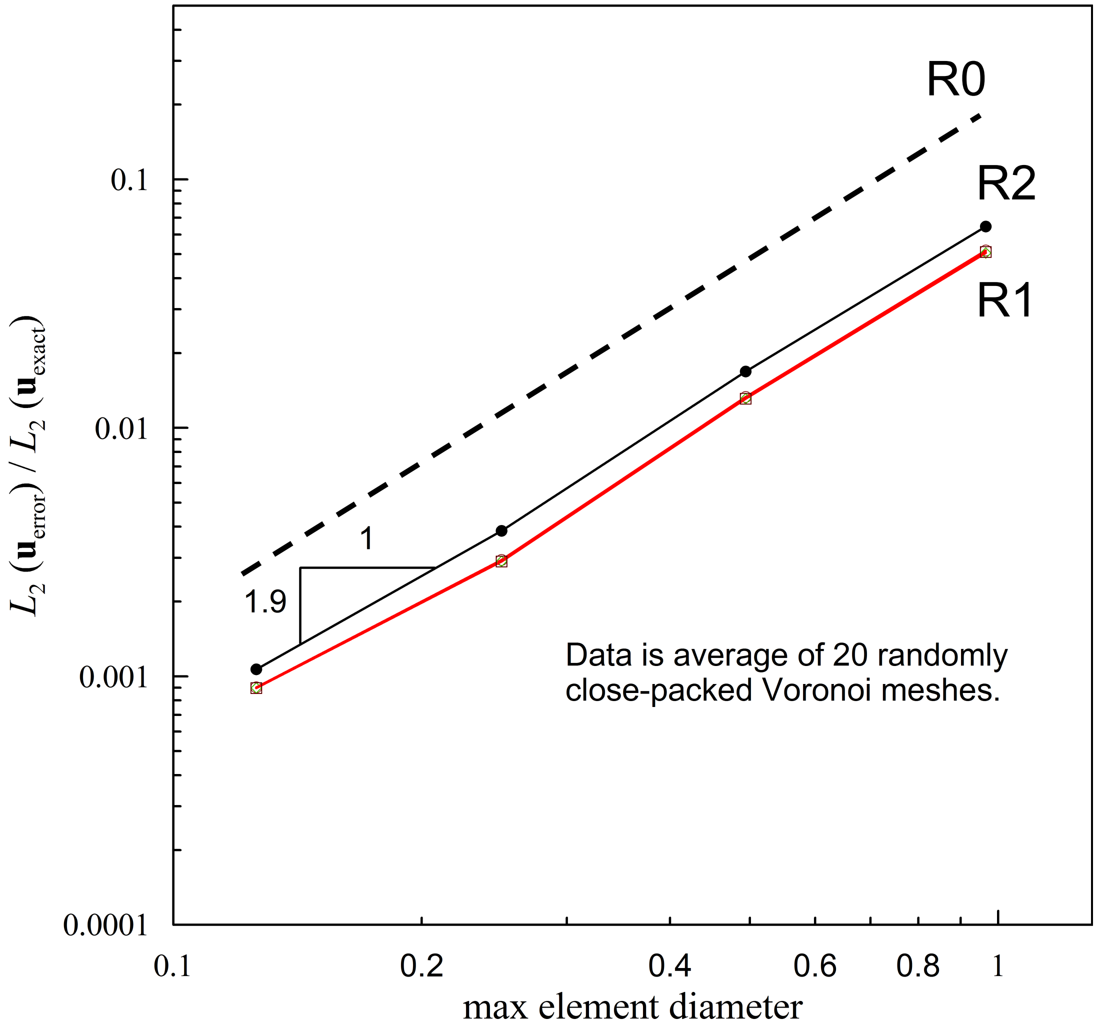

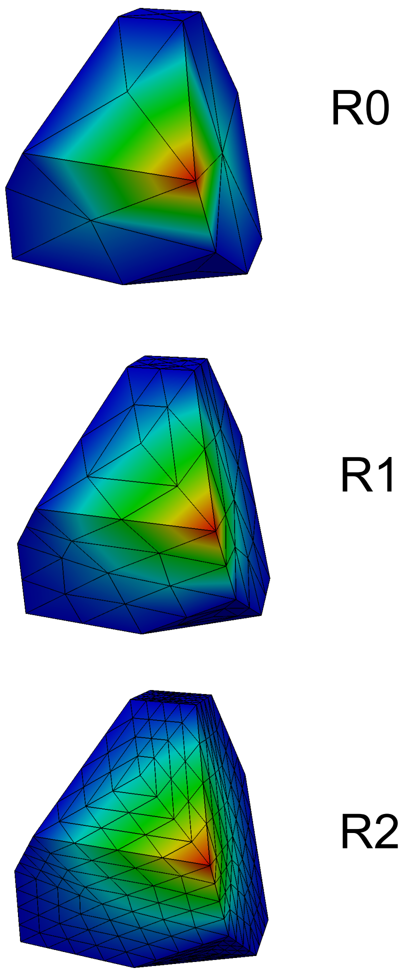

Dynamic Mesh Connectivity

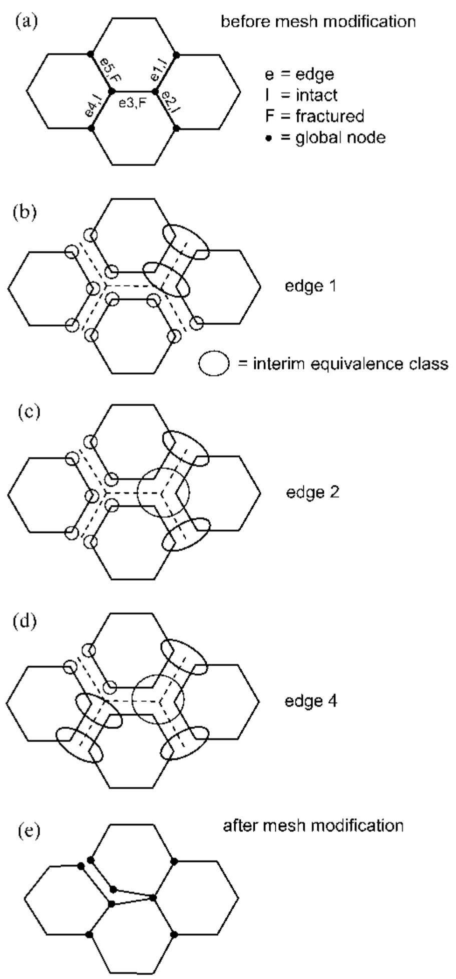

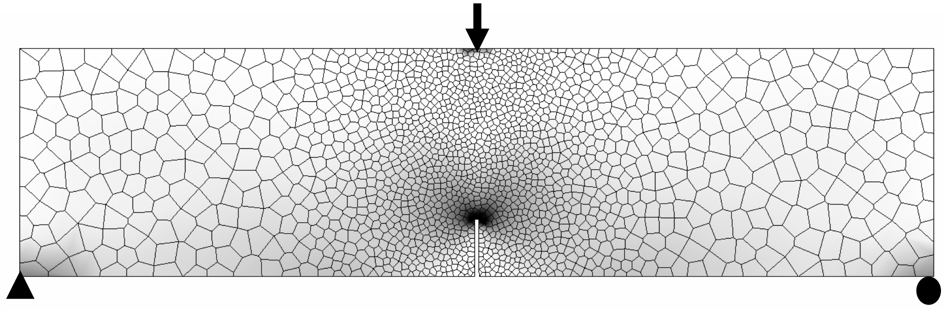

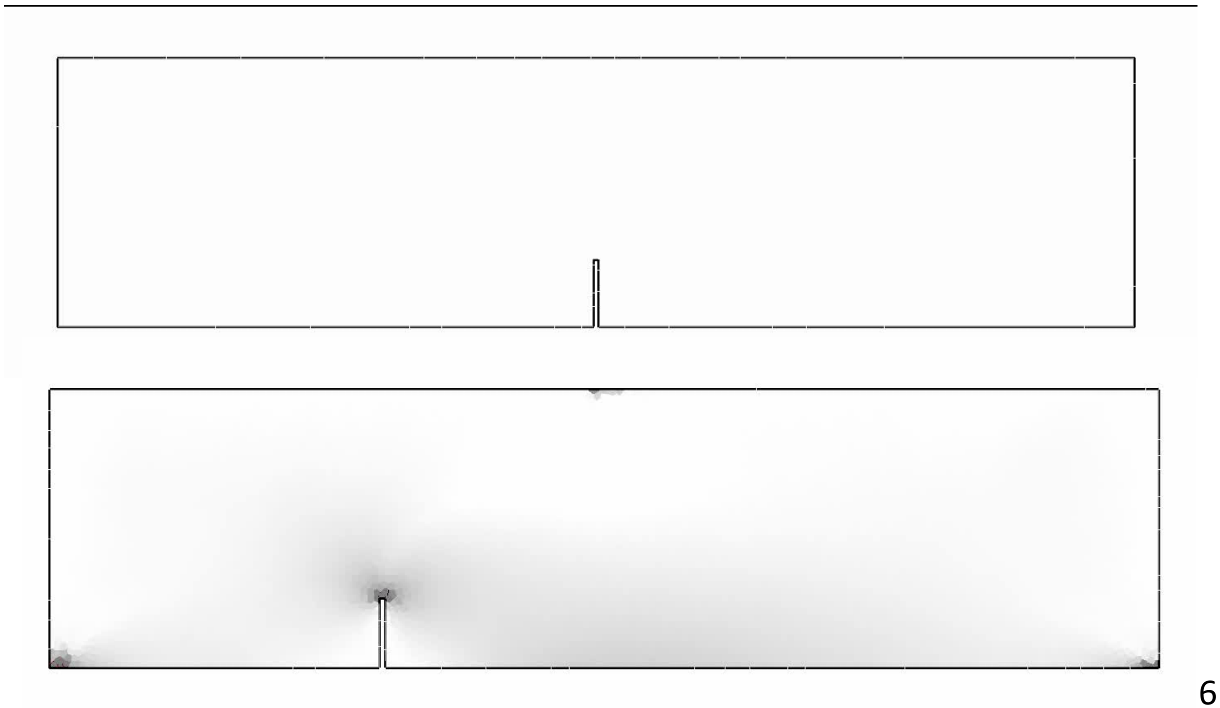

Quasi-Brittle Material Impact

(Bishop, J., 2009, *Computational Mechanics*, v. 44)

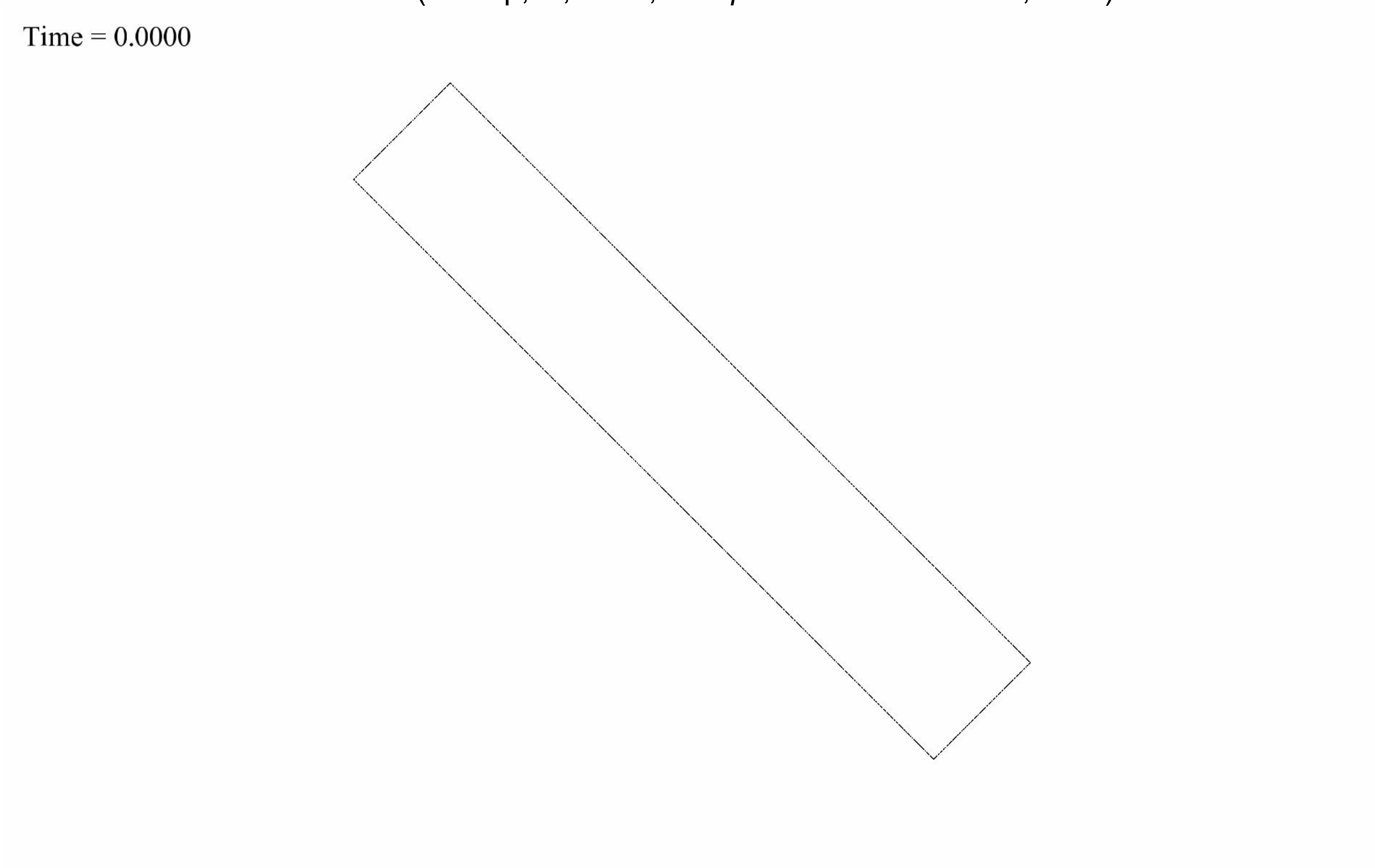

Impact Example

(Bishop, J., 2009, *Computational Mechanics*, v. 44)

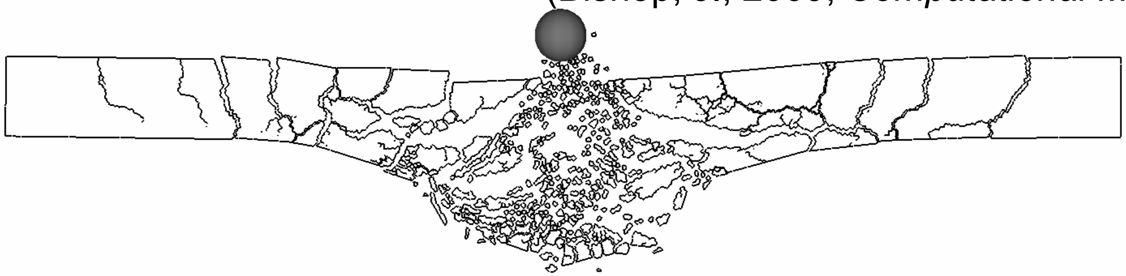

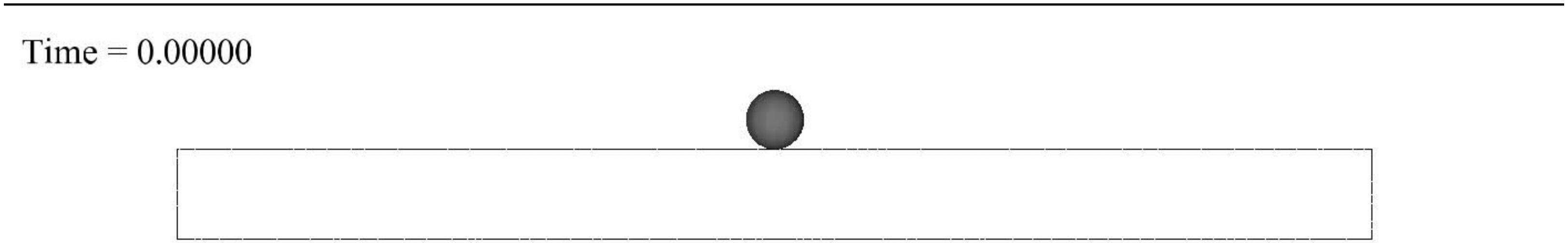

CFSES: Center for Subsurface Energy Security

Sandia National Laboratories

(www.utcfses.org)

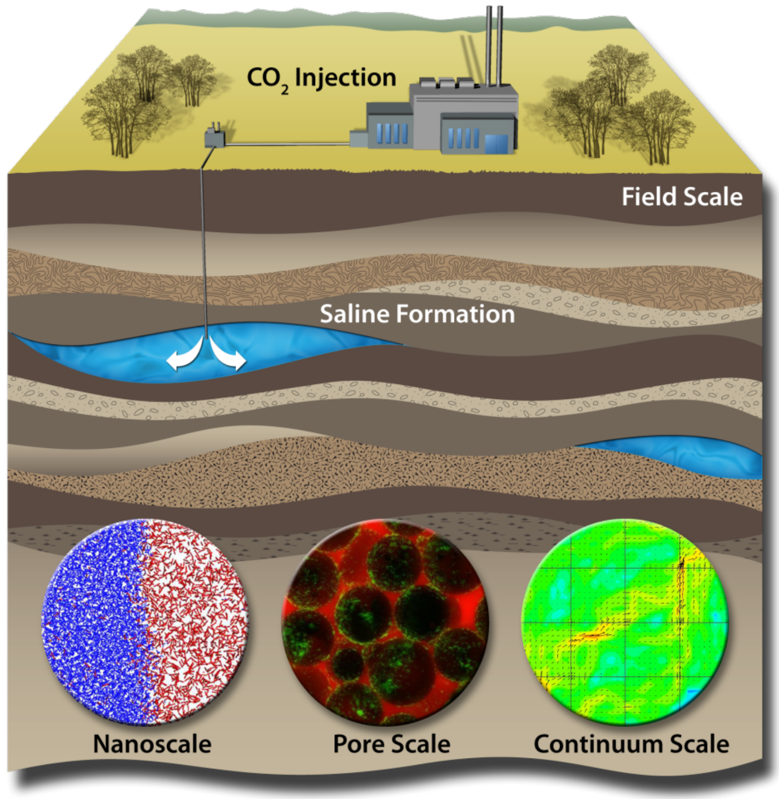

10^3 years (or more)

Time

10^{-15} second

10^{-9} m	10^{-5} m	10^{-1} m	10^{2} m
Focus Area 1	**Focus Area 2**	**Focus Area 3**	**Focus Area 4**
Nanoscale	Pore Scale	Continuum Scale	Field Scale

Potential Leakage Paths for CO_2

Primary CO_2 trapping mechanism is structural.

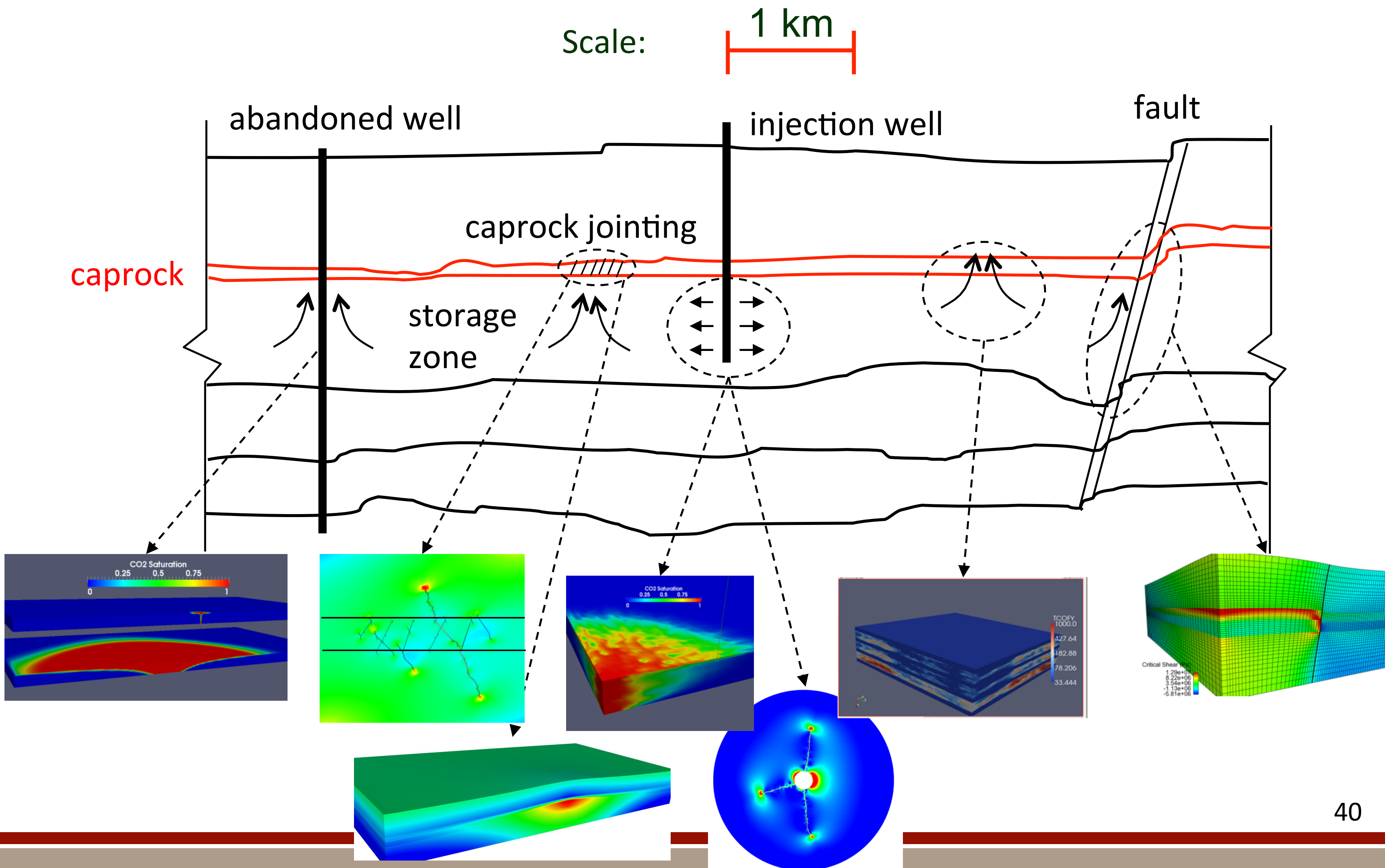

Hydromechanical Coupling in Fractured Rock

bulk constitutive properties

(Sandia GeoModel
Fossum & Brannon, 2004)

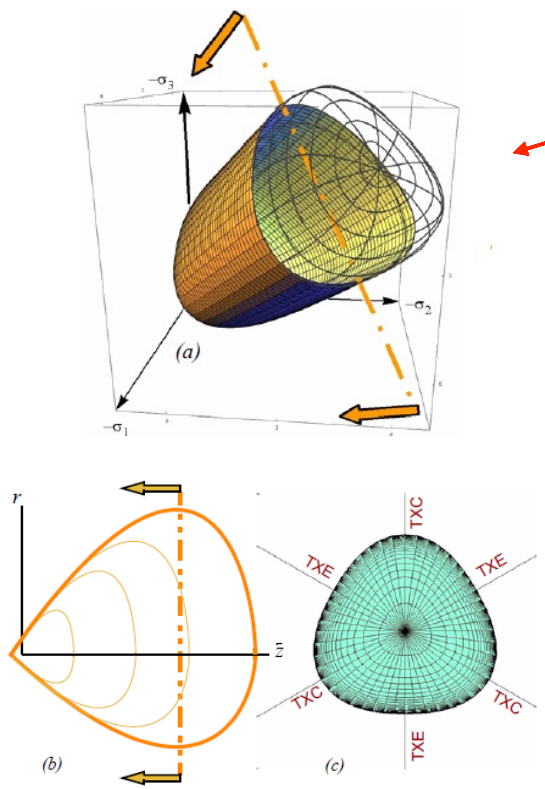

Fractured Porous Rock

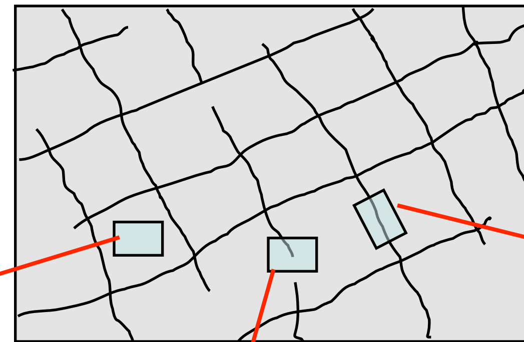

fracture contact properties

$$\sigma'_n = \sigma_n - p$$

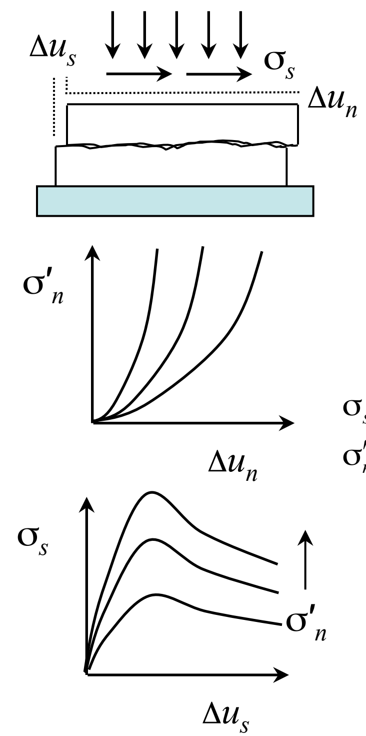

$$\sigma_s = \sigma_s\{\Delta u_s, \Delta u_n\}$$
$$\sigma'_n = \sigma'_n\{\Delta u_s, \Delta u_n\}$$

crack-tip cohesive properties

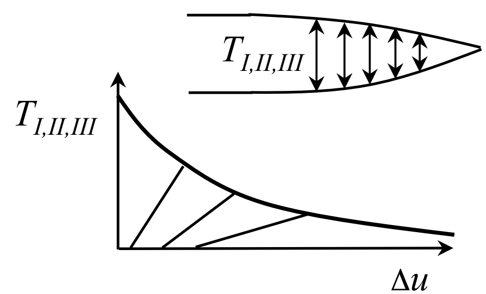

additional challenges

- scale dependence
- history dependence
- precipitation
- dissolution

MeshingGenie (Trilinos)

(Ebeida, M., Knupp, P., Vitus Leung, Sandia National Laboratories)

Fractured Rock

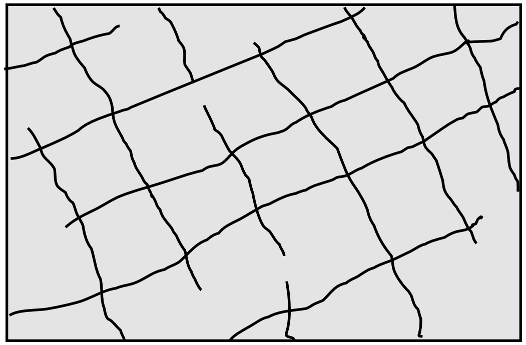

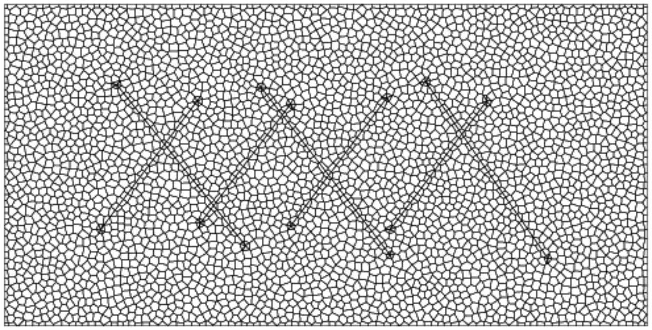

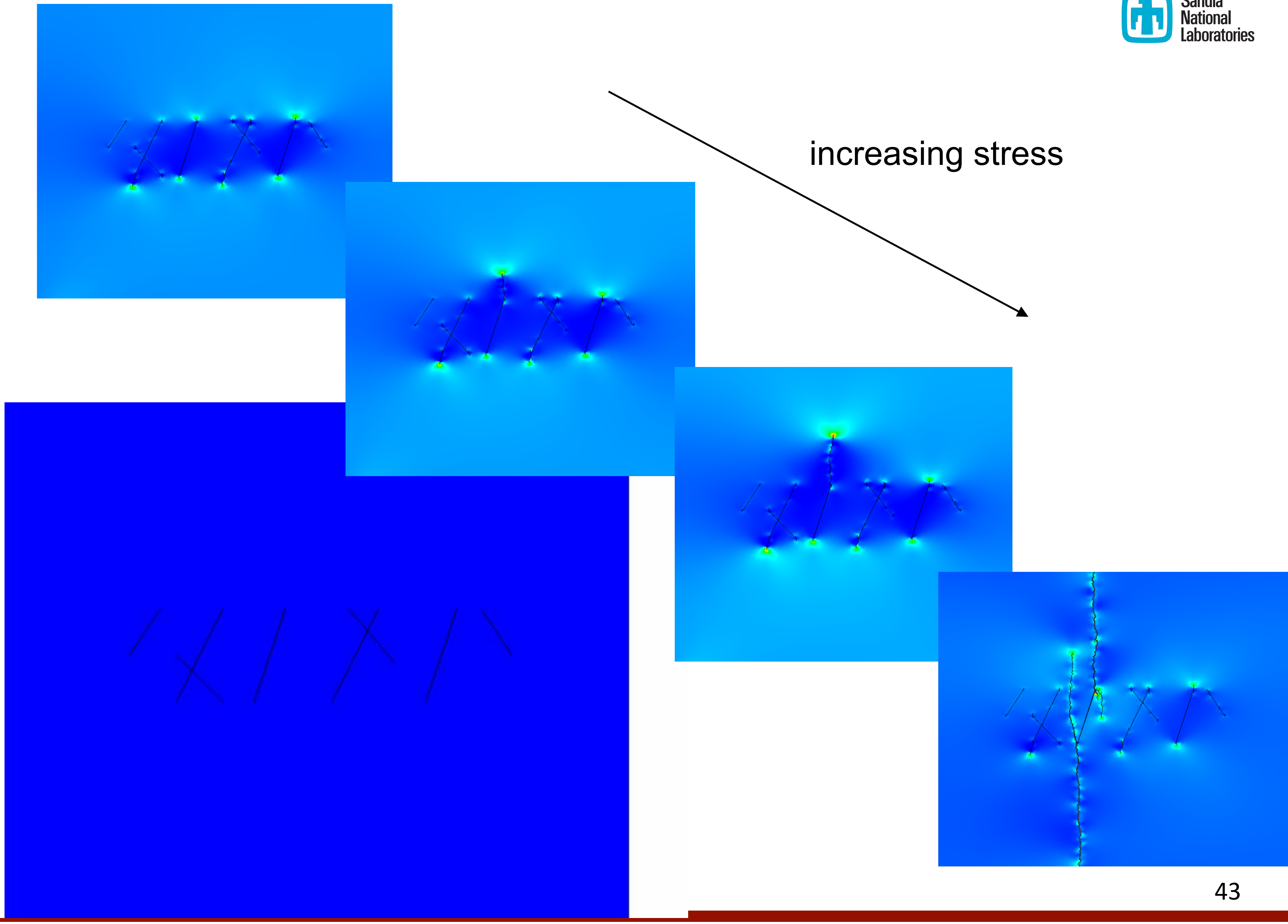
increasing stress

Fluid Flow in 2D Discrete Fracture Networks

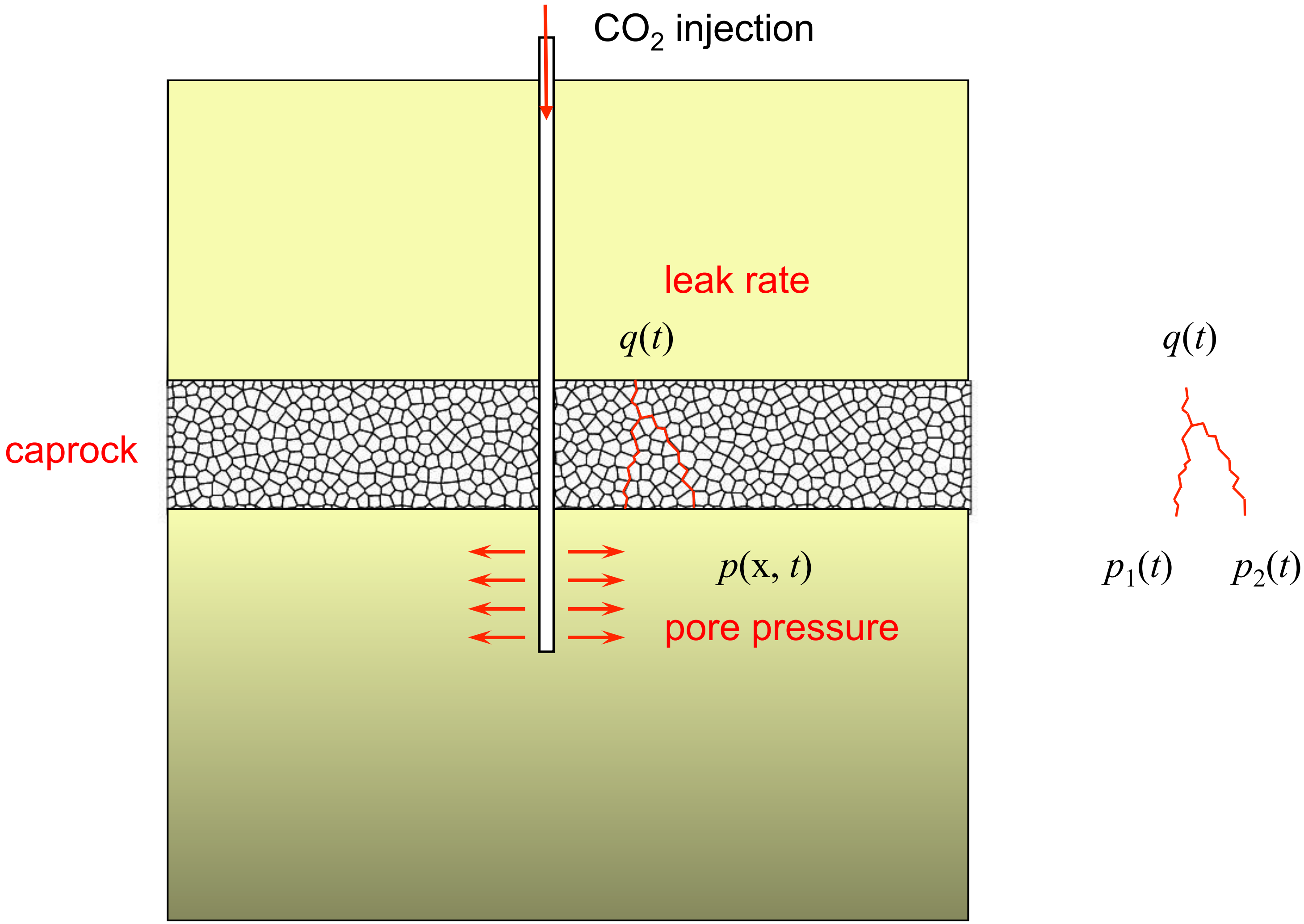

Fluid Flow in 2D Discrete Fracture Networks

Solve fluid network to get nodal pressures and flow rates.

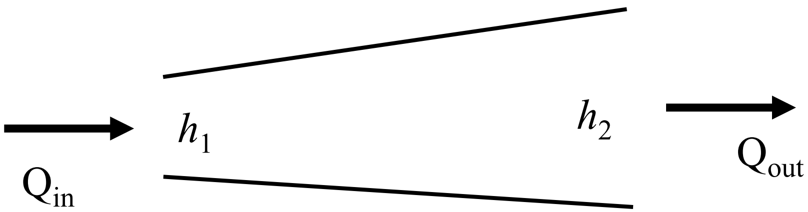

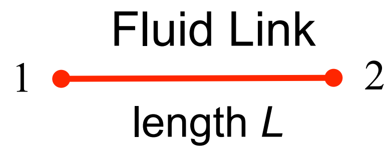

$$\begin{Bmatrix} Q_1 \\ Q_2 \end{Bmatrix} = \frac{T}{\mu}\begin{bmatrix} 1 & -1 \\ -1 & 1 \end{bmatrix}\begin{Bmatrix} P_1 \\ P_2 \end{Bmatrix}$$

$$T = \frac{h_1^2 h_2^2}{6L}\frac{1}{h_1 + h_2}$$

Q = flow rate
P = pressure
μ = viscosity
T = transmissibility

Reynold's lubrication equation

$$\nabla(\rho\mathbf{Q}) = 0$$

$$\mathbf{Q} = -\frac{h^3}{12\mu}(\nabla p - \rho g h)$$

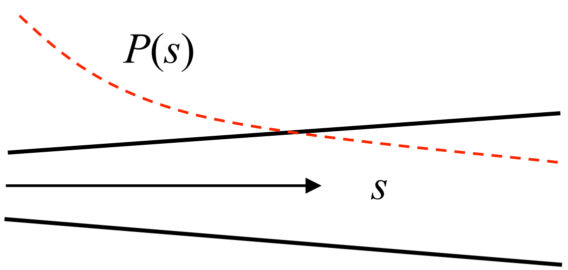

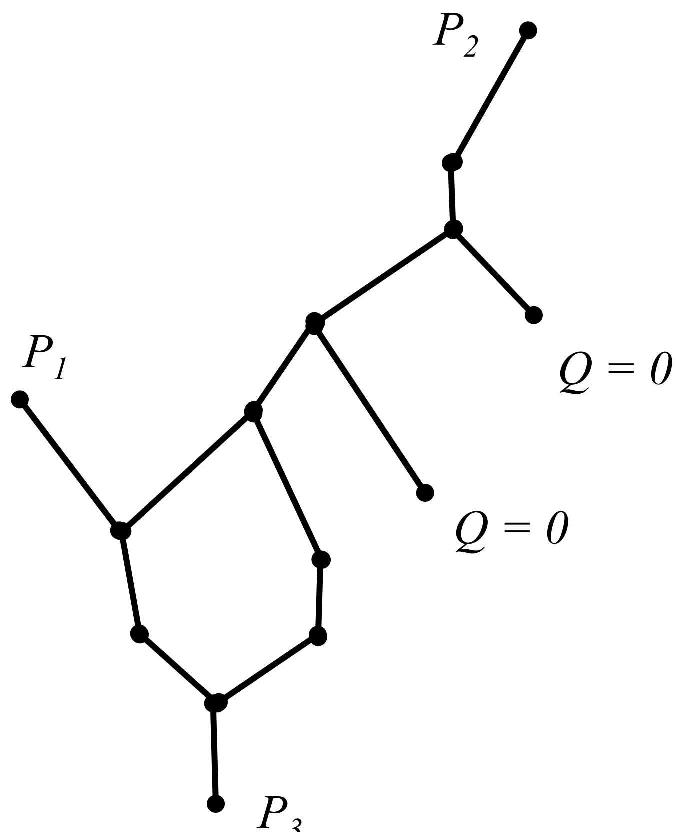

Fluid Flow in Discrete Fracture Networks

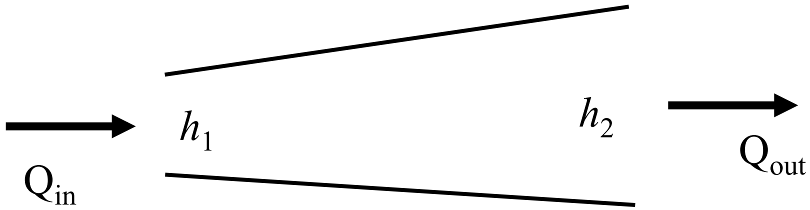

Reynold's lubrication equation

$$\nabla(\rho \mathbf{Q}) = 0$$

$$\mathbf{Q} = -\frac{h^3}{12\mu}(\nabla p - \rho g h)$$

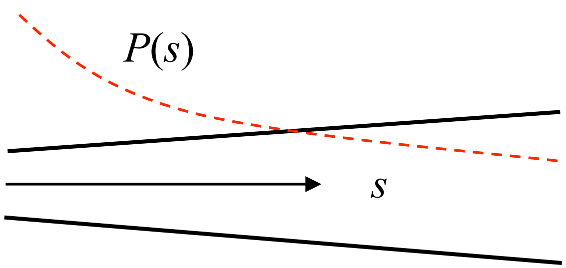

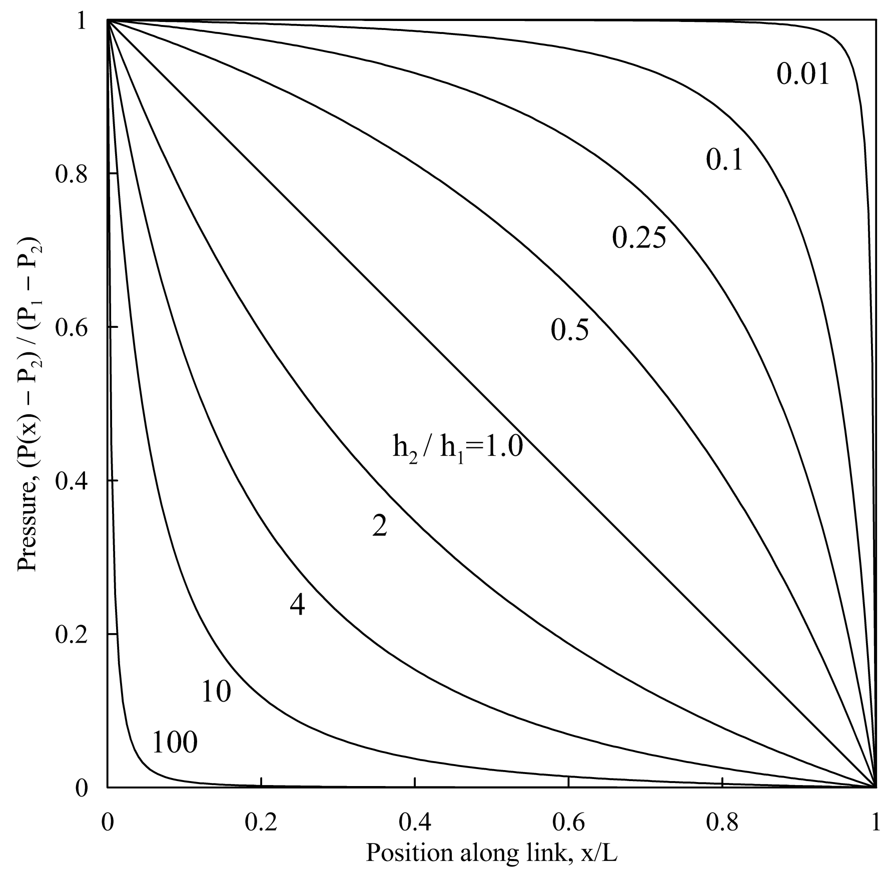

Hydraulic Fracture Simulation

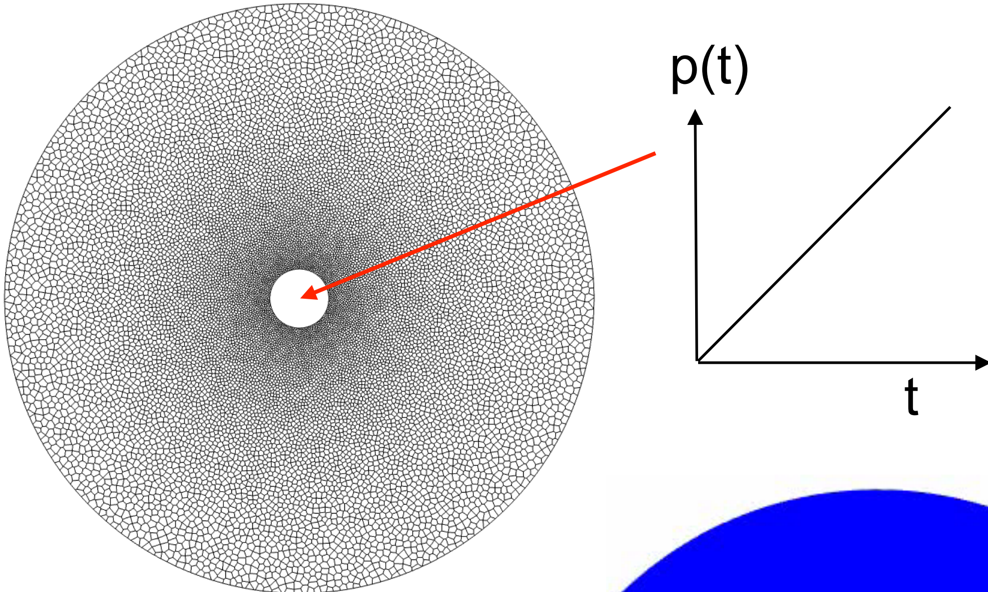

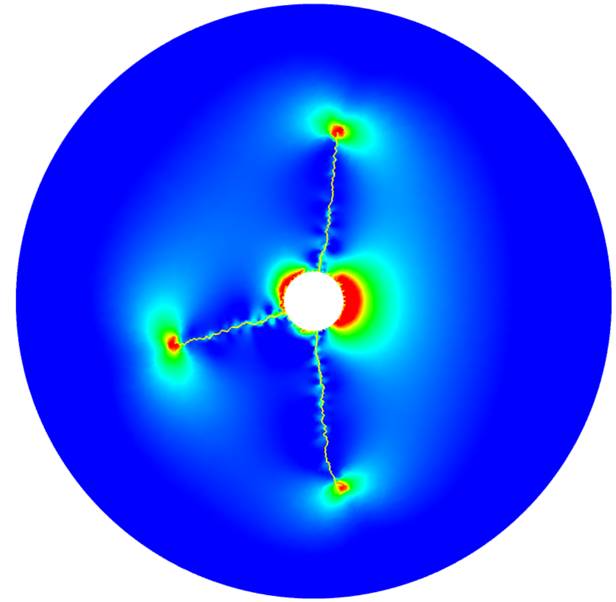

Coupled fluid flow in fracture networks

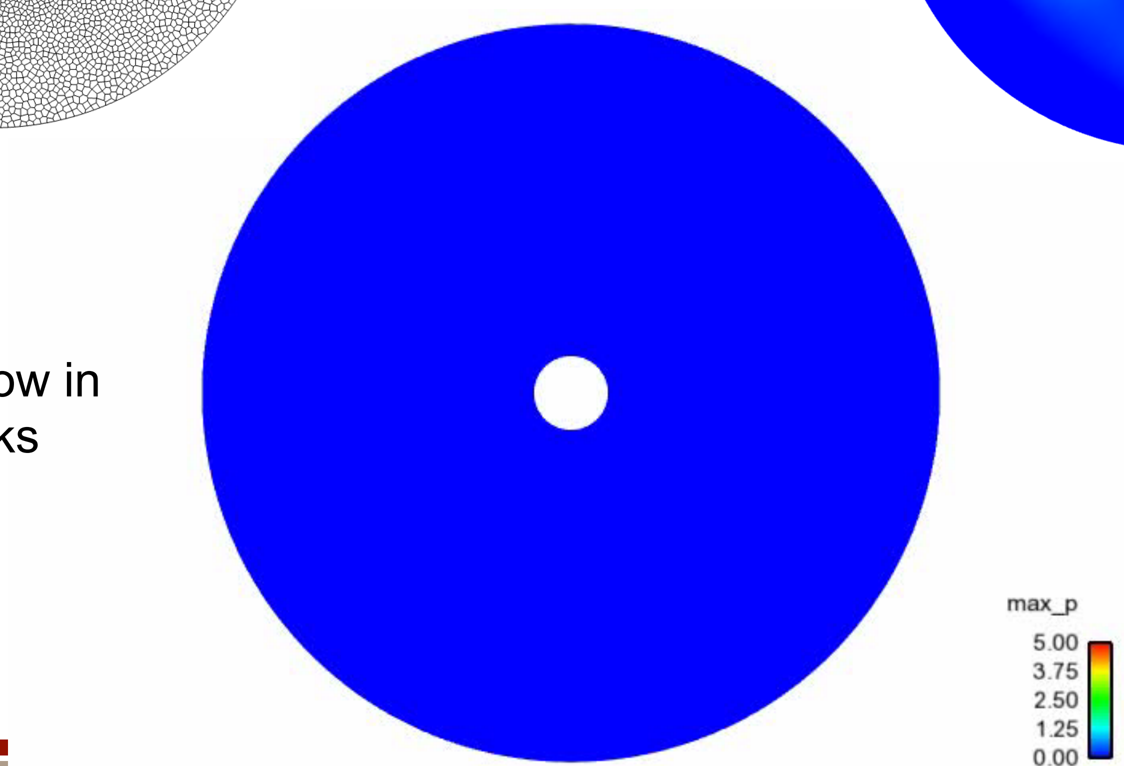

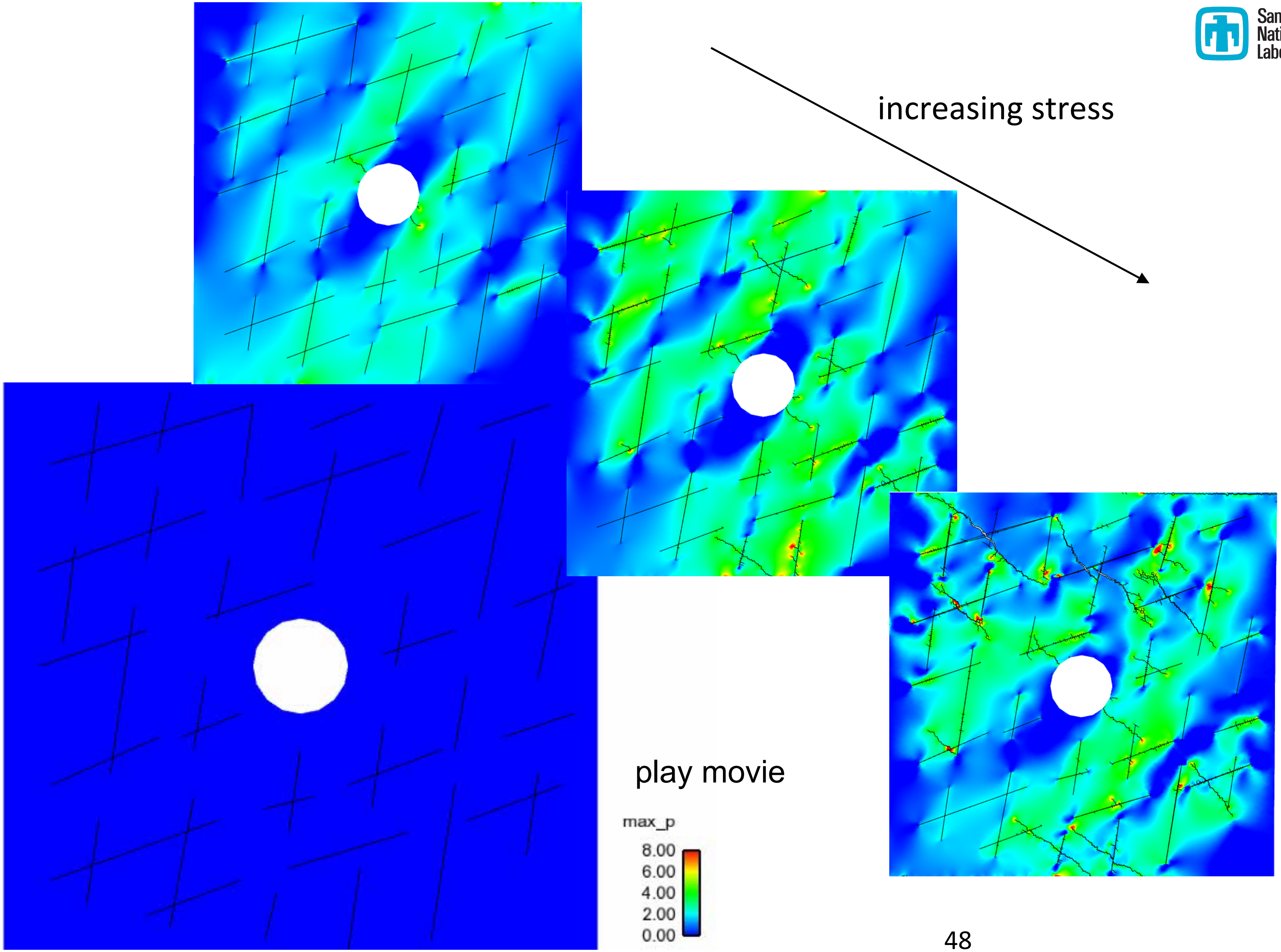

48

Outline

1. Pervasive fracture and fragmentation
2. Random meshes and a polyhedral finite-element formulation
3. Assessing mesh convergence in a probabilistic sense
4. Summary

(Bishop, J. and Strack, O., 2011, *IJNME*, v. 88)

Example: Explosively Loaded Cylinder

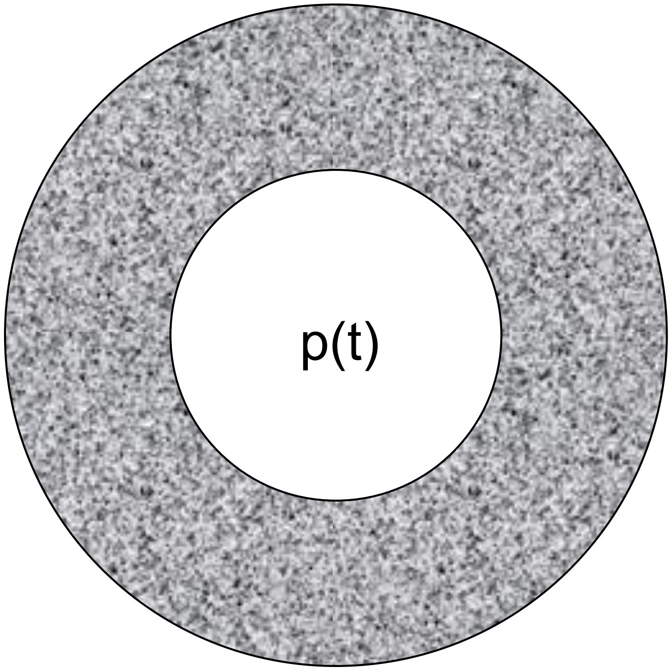

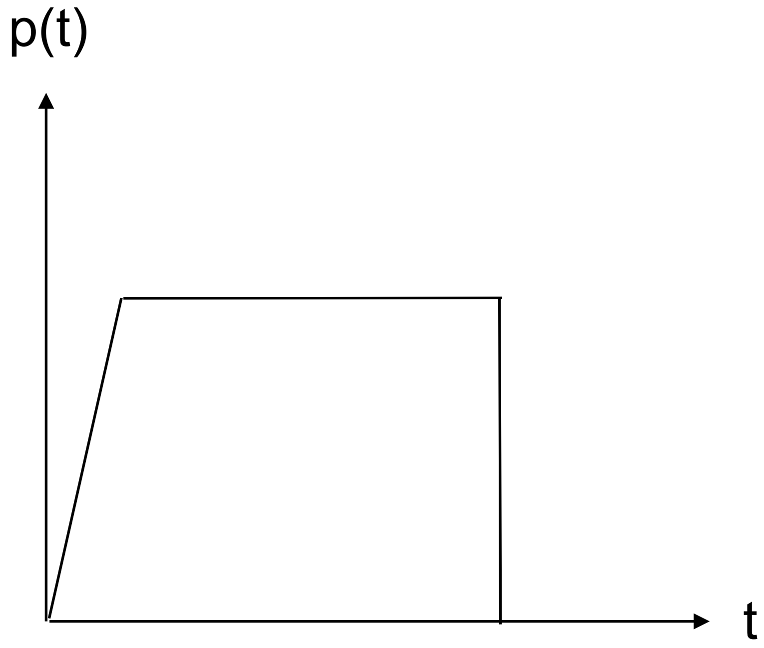

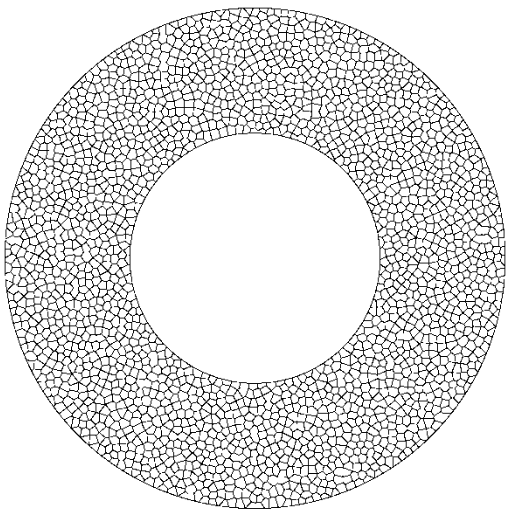

t = 0

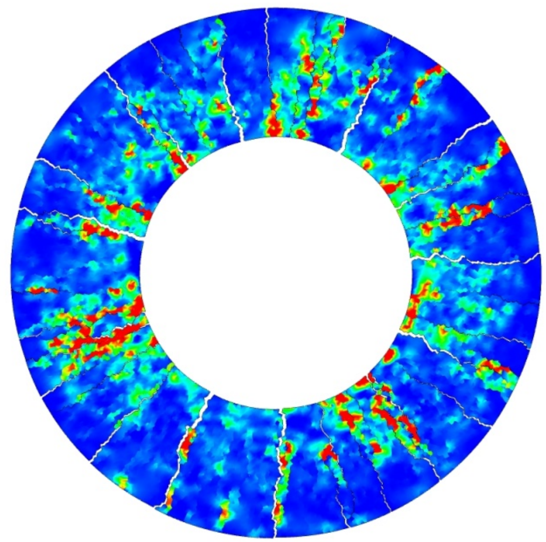

t = 2 ms

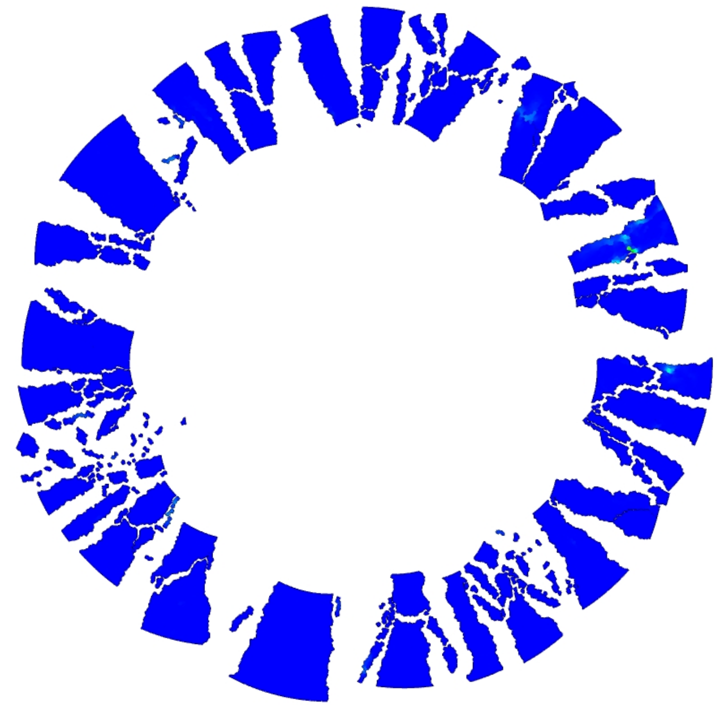

t = 20 ms

realization 1

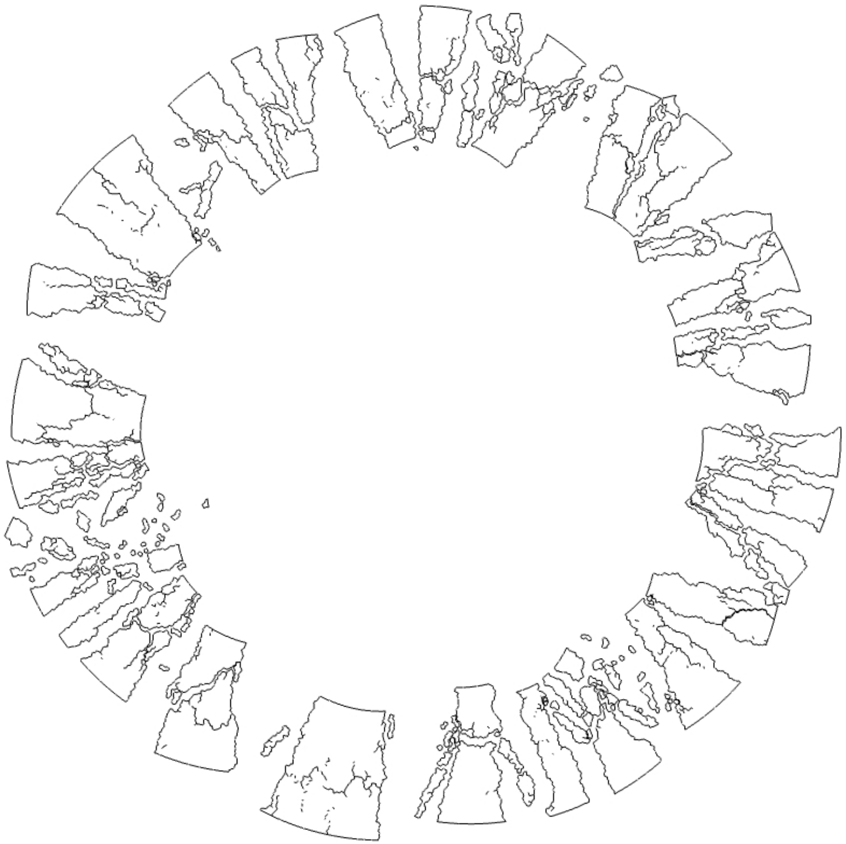

realization 2

Mesh Convergence?

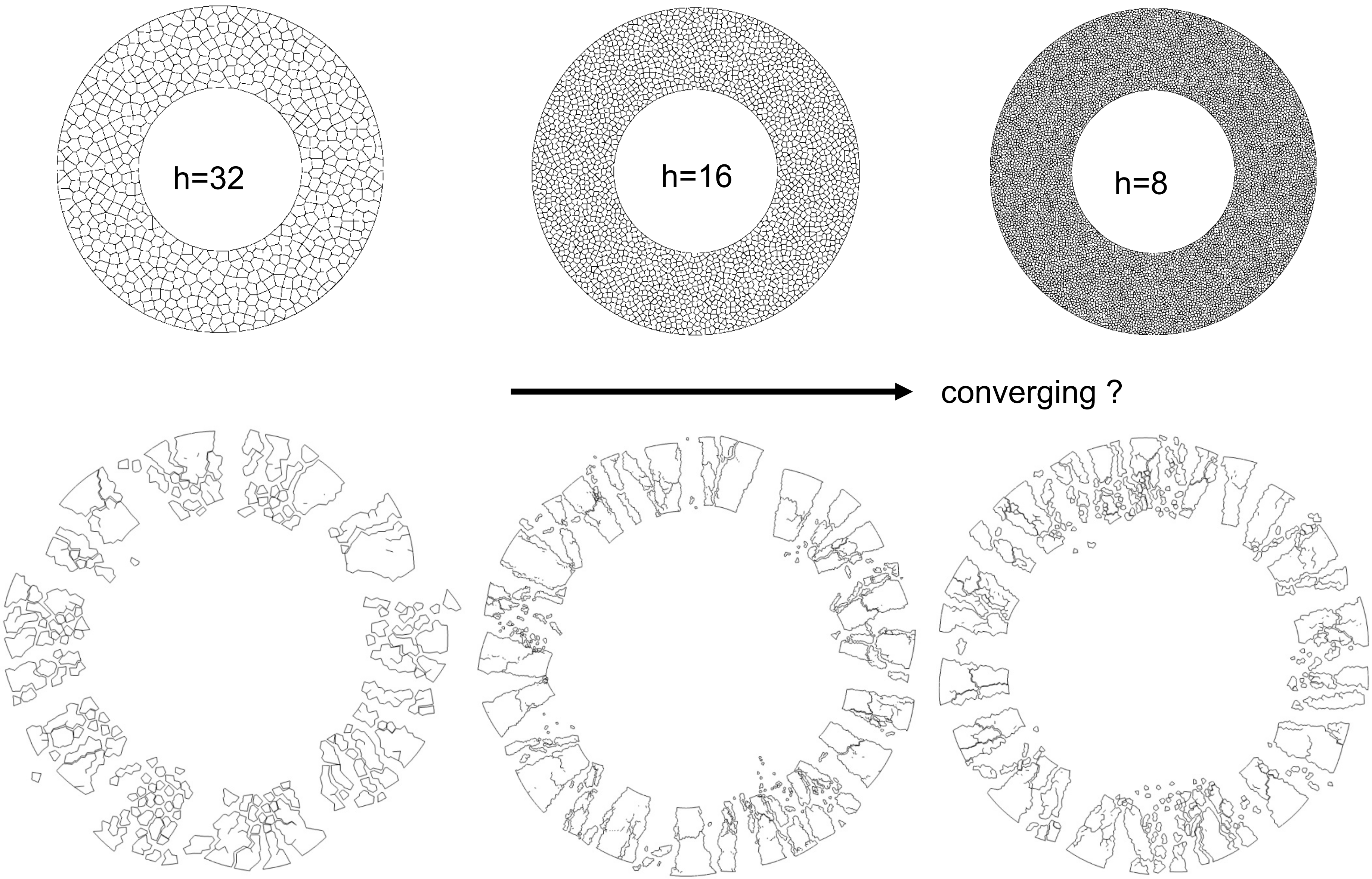

Review of Probability

X = random variable

(an engineering quantity of interest)

PDF

$f(x)$ probability distribution function

$$f(x) = \frac{dF}{dx}$$

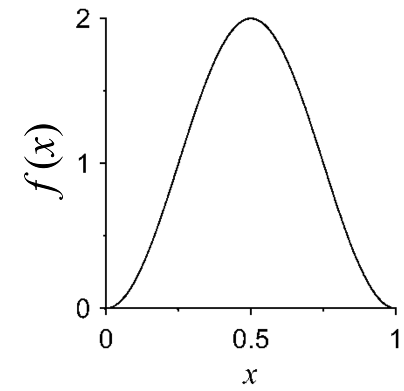

CDF

$F(x)$ cumulative distribution function

$$F(x) = \Pr(X < x)$$

$$F(x) = \int_{-\infty}^{x} f(x')\,dx'$$

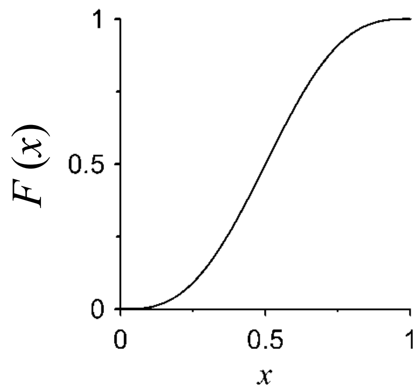

Definitions of Statistical Convergence

almost sure convergence

$$\Pr\left(\lim_{h\to 0} x_h = x\right) = 1$$

convergence in r-mean

$$\lim_{h\to 0} E\left(\left|x_h - x\right|^r\right) = 0$$

convergence in probability

$$\lim_{h\to 0} \Pr\left(\left|x_h - x\right| > \varepsilon\right) = 0$$

convergence in distribution

$$\lim_{h\to 0} F_h(x) = F(x)$$

increasing strength

Example

sequence of random variables X_n, $n = 1, 2, 3, \ldots$

PDF

$$f_n(x) = 1 - \cos(2\pi n x)$$

CDF

$$F_n(x) = x - \frac{1}{2\pi n}\sin(2\pi n x)$$

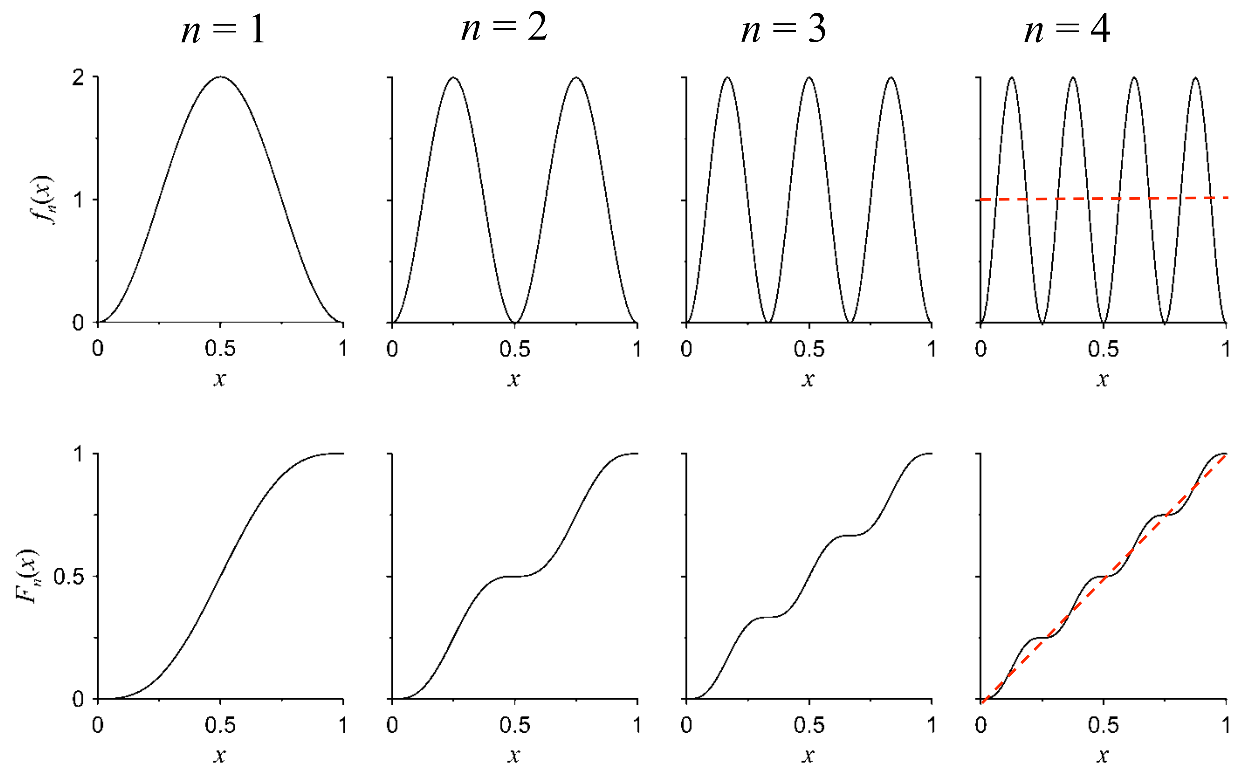

YES convergence-in-distribution: $\lim_{n\to\infty} F_n(x) = x$ for each x (pointwise)

NO convergence-in-probability: $\lim_{n\to\infty} \Pr\left(|X_n - X| > \varepsilon\right) \overset{?}{=} 0$ $\Pr\left(|X_n - X| > \varepsilon\right) = \frac{2}{\pi} + O(\varepsilon)$

for all n

How to Assess Convergence-in-Distribution?

$$\lim_{h \to 0} F_h(x) \stackrel{?}{=} F(x)$$

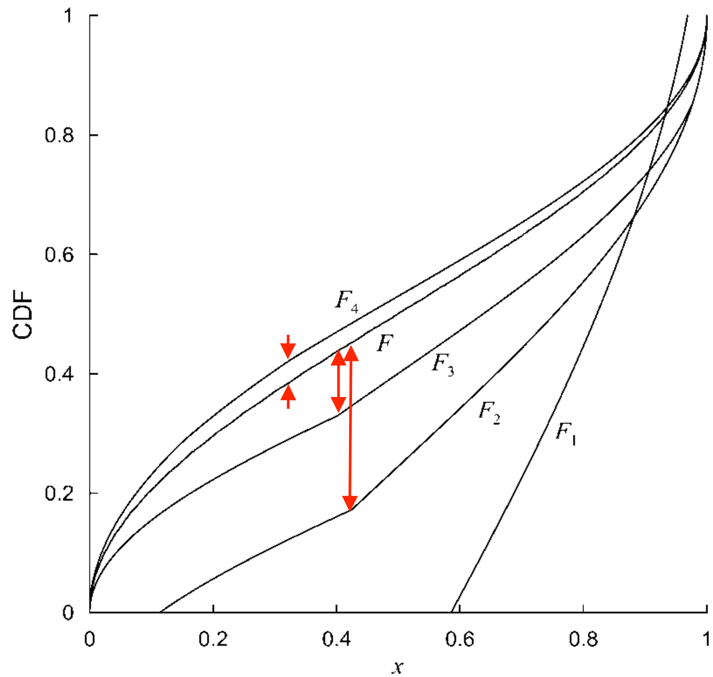

engineering quantity-of-interest

use L_∞ norm: $$L_\infty(F_h, F) = \sup_x |F_h(x) - F(x)|$$

What about finite sampling effects?

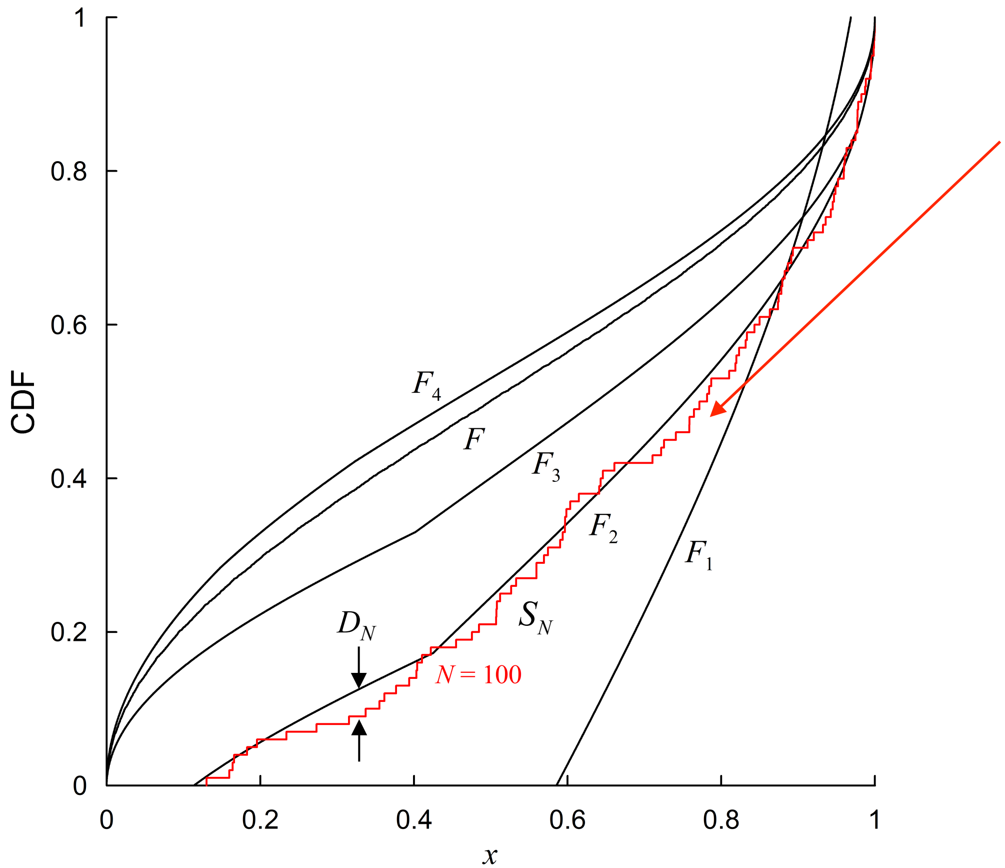

empirical CDF, $S_N(x)$

$$S_N(x) \equiv \begin{cases} 0, & x < x_1 \\ \dfrac{r}{N} & x_r < x < x_{r+1} \quad r = 1, \ldots, N-1 \\ 1 & x_N < x \end{cases}$$

Strong Law of Large Numbers:

$$\lim_{N \to \infty} S_N(x) = F(x) \quad \text{(almost surely)}$$

Finite Sampling Fluctuations in CDF

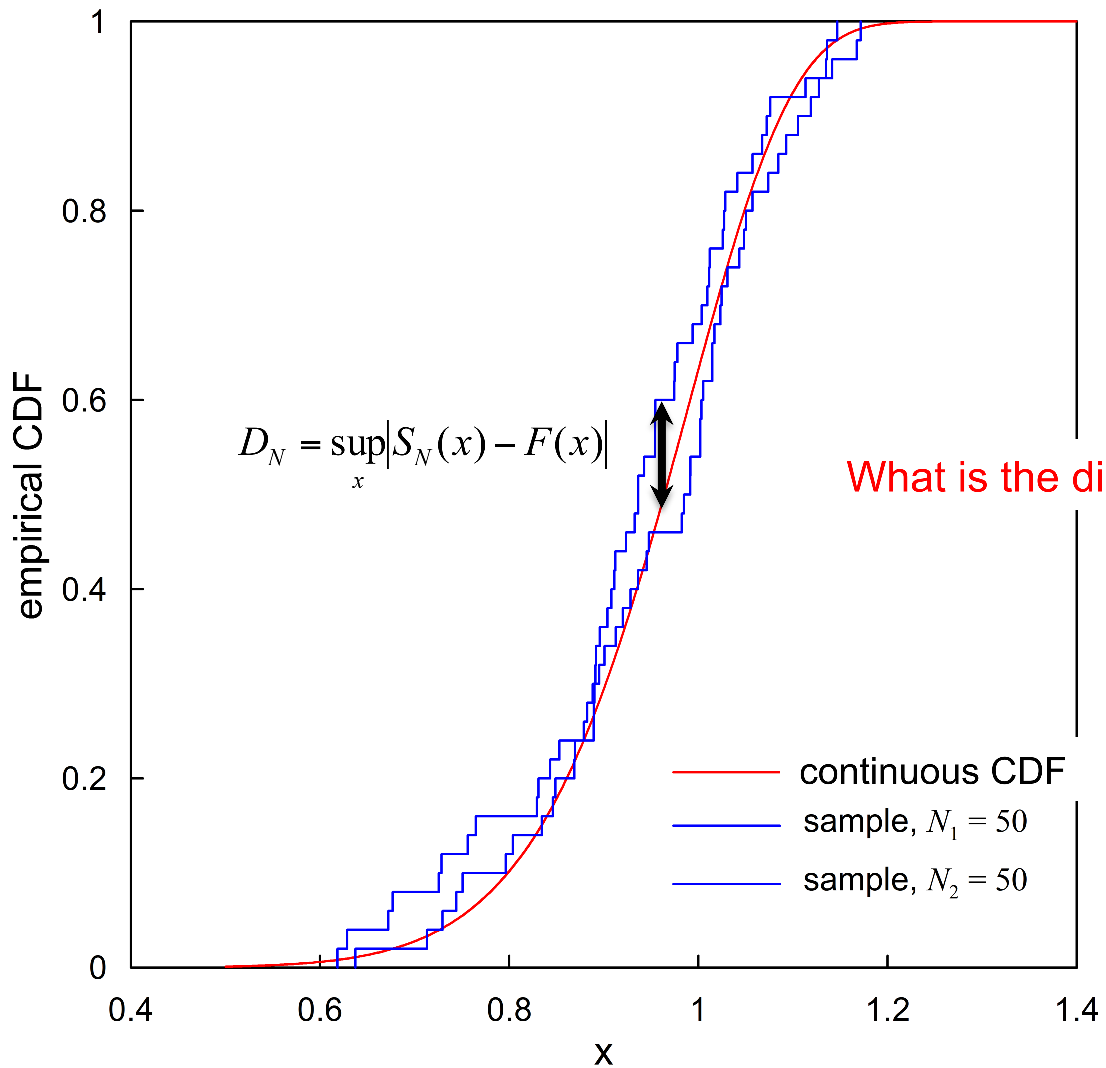

What is the distribution for D_N?

Kolmogorov-Smirnov Statistic

$$D_N = \sup_x \left| S_N(x) - F(x) \right|$$

$$\lim_{N\to\infty} \Pr\left(D_N < z/\sqrt{N}\right) = 1 - 2\sum_{j=1}^{\infty} (-1)^{j-1} \exp(-2j^2 z^2) \equiv p(z)$$

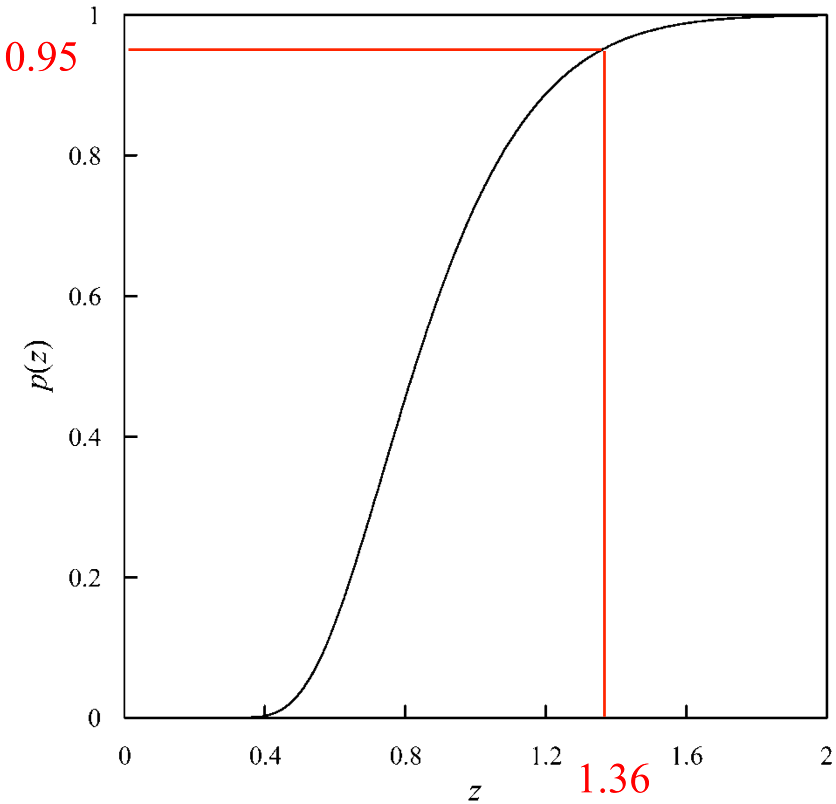

$$\left.\begin{array}{l} \Pr\left(D_N < \dfrac{1.63}{\sqrt{N}}\right) = 99\% \\ \Pr\left(D_N < \dfrac{1.36}{\sqrt{N}}\right) = 95\% \\ \Pr\left(D_N < \dfrac{1.19}{\sqrt{N}}\right) = 90\% \end{array}\right\}$$ confidence bounds

- independent of distribution
- only for continuous CDFs

(conservative to within 2% for $N > 50$)
(tabulated for $N < 50$)

Kolmogorov-Smirnov Statistic

95% confidence bounds

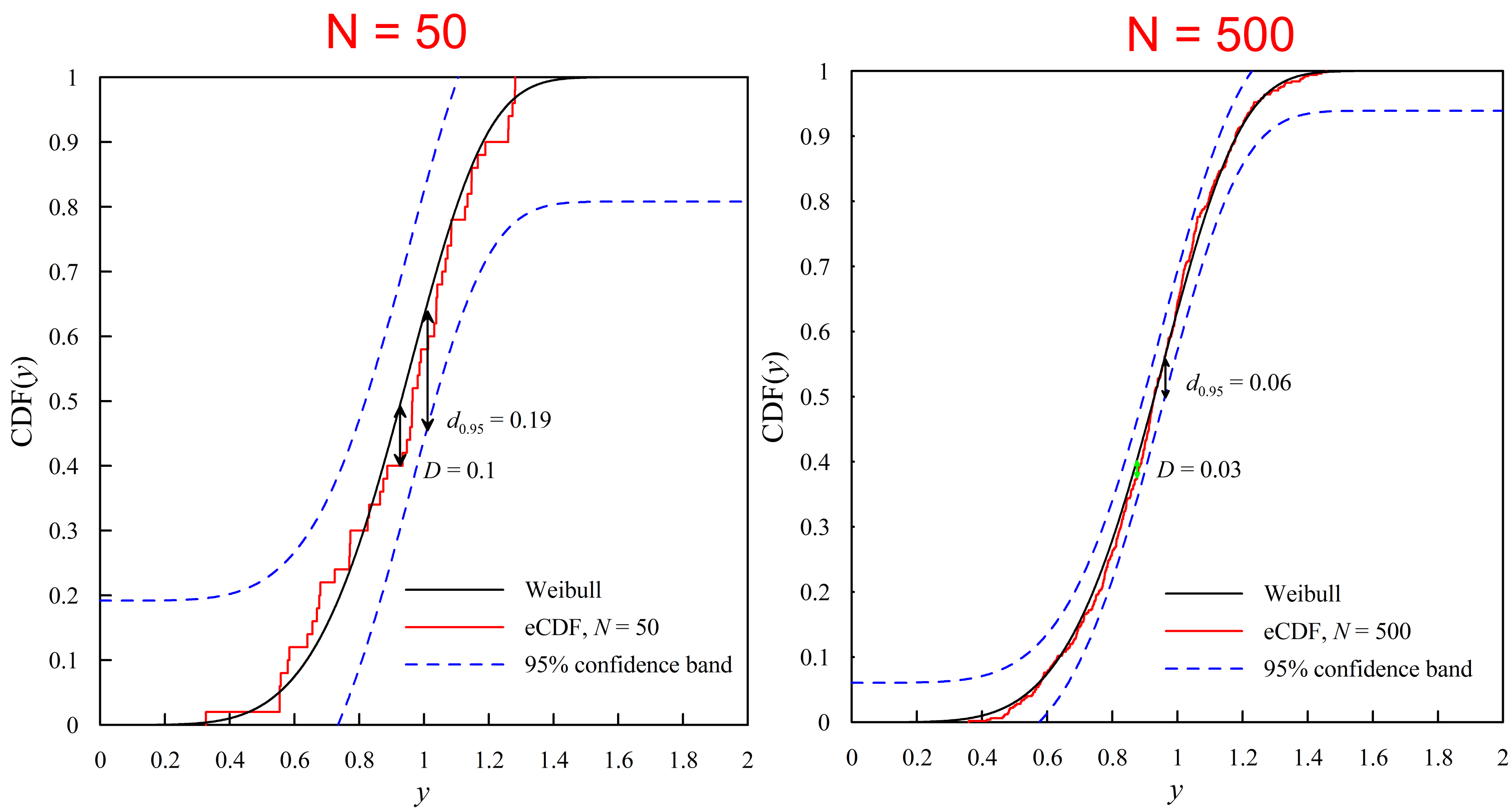

How to use KS-statistic to assess convergence-in-distribution with finite sample sizes?

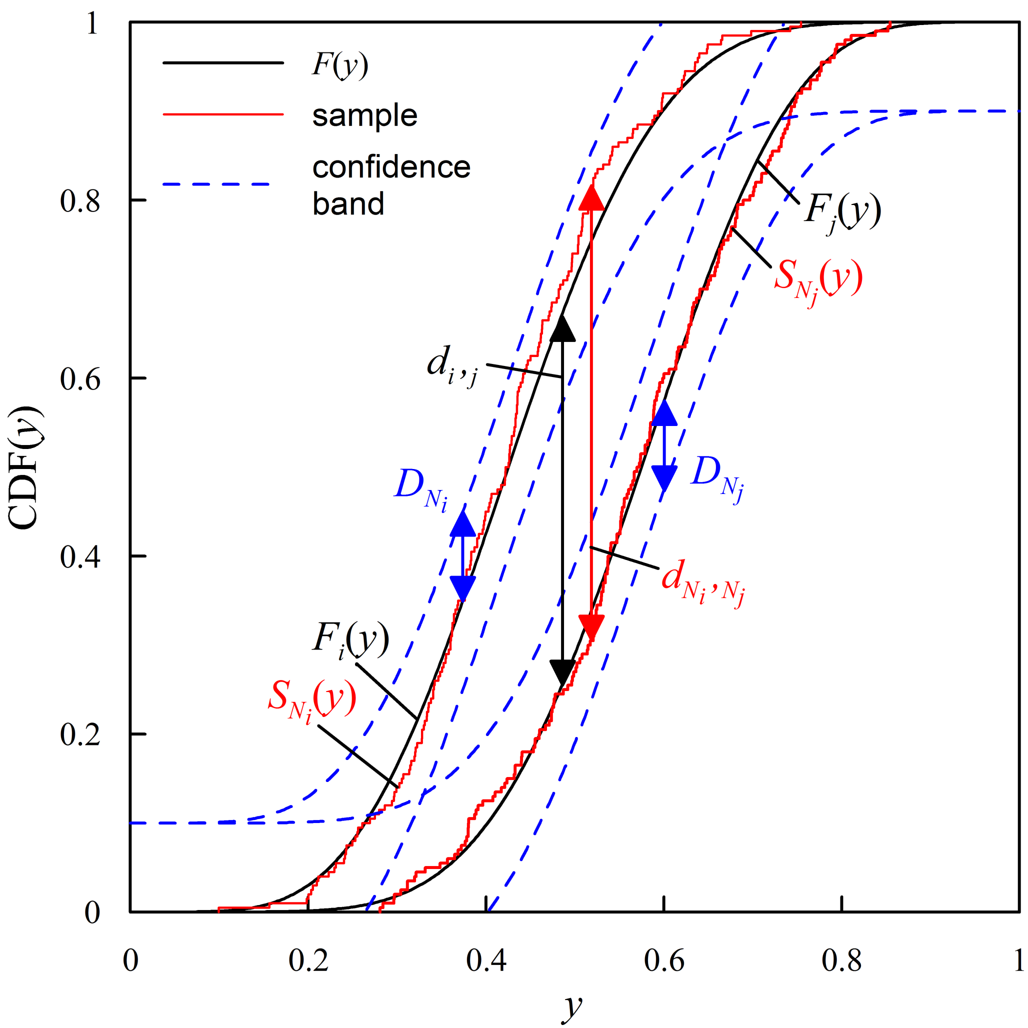

$$\left| d_{i,j} - d_{N_i,N_j} \right| \leq D_{N_i} + D_{N_j} = \frac{z_i}{\sqrt{N_i}} + \frac{z_j}{\sqrt{N_j}}$$

(Bishop, J. and Strack, O., 2011, *IJNME*, v. 88)

Summary

1. Presented a finite-element method for modeling pervasive fracture in materials and structures based on random meshes.
2. Presented a polyhedral finite-element formulation for both convex and nonconvex elements.
3. If engineering quantities-of-interest are extremely sensitive to initial conditions and system parameters, need to embrace a probabilistic description.
4. Presented a statistical-method for verifying and validating nonlinear dynamical systems in this regime including pervasive fracture.